Development of Operation Training System and Improvement of Operation Interface for Improving Operators' Skills of Hydraulic Excavators

(油圧ショベルのオペレータの操作スキル向上を目的とした
操作トレーニングシステムの開発と操作インターフェースの改善)

by

Ryota SEKIZUKA

Graduate School of Engineering

Hiroshima University

March, 2022

Contents

List of Figures

List of Tables

Chapter 1

Introduction

1.1 Background and Purpose

In recent years, the automation of various machines advanced by the development of technologies such as artificial intelligence and the internet of things. However, the scene in which humans mainly operate machines from complexity and diversity of the work such as surgical robots and construction machines also remains. The operation of these machines is often special, and advanced skill is required in order to operate at will. For example, the operation of a hydraulic excavator, which is a typical construction machine, is complicated since it is necessary to operate four joint motions using two levers simultaneously. As a means of operation skill improvement of the operator, operation training and operability improvement of the machine are mentioned. There is a case in which the problem in cost and safety arises when the operation training is carried out using the real machine. The environment in which safety training can be carried out at low cost such as a simulator is effective. Quantitative evaluation of operation skills is also important for operation training. By digitizing the operation skill and visualizing the proficiency of the operator, the optimum training in proportion to the proficiency is possible. On the other

hand, it is also important to improve the machine's operability because extra time is required for the mastery of the operation when the operability is bad. As a means of improving the operability, optimization of the machine control, partial assist of the operation, and improvement of the operation interface are mentioned. The skill required for operation can be reduced by adopting these techniques.

This study focuses on hydraulic excavators, which are used in many cases among machines operated by humans. We aim at the operation skill improvement of the operator from three viewpoints: developing a safe training environment at low cost, quantitative evaluation of the operation skill, and improvement of the operation interface. Hydraulic excavators are representative construction machinery, and they occupy about half of the construction machinery market in Japan. As a countermeasure to the productivity lowering caused by the labor shortage in the construction industry, it is important to offer a training environment that can safely raise the operator at a low cost and improve the operation interface of the hydraulic excavator.

This dissertation addresses the following topics:

- Development of the operation training system of hydraulic excavator

- Verification of operation skill evaluation indices of hydraulic excavator

- Force feedback design of operation levers to improve hydraulic excavator operability

The first topic is the development of low cost and safe operation training system for hydraulic excavators. Operation training with a real excavator may be difficult due to cost and safety issues. Simulators can be effective for training in situations wherein it is difficult to train using an actual machine in

a real environment. Training can be performed safely by using a simulator and with lower operating cost than that incurred when using the actual machine. However, there exists a challenge in the case of excavator simulators: It is difficult to reproduce the behavior of soil excavated in real time because of the calculation cost. We think that this problem can be solved by using a training system using an remote controlled (RC) toy excavator. However, a general RC toy excavator is not suitable for training because the viewpoint and operation system are different from the real excavator. In this study, we developed a by using an RC toy excavator and virtual rearity (VR) technology with the same viewpoint and operating interface as a real excavator.

The second topic is the verification of operation skill evaluation indices of a real excavator by the training system which we developed. It is important to visualize an operator's proficiency level by quantitatively evaluating operation skills in operation training. However, it is unclear whether the skill evaluation indices used in the real excavator can be applied when using the RC toy excavator that does not completely reproduce the characteristics of the real excavator. We verify the indices which can evaluate the operation skill of the real excavator using the proposed system.

The third topic is the force feedback design of operation levers to improve hydraulic excavator operability. Various studies on the feedback of the machine information as one of the improvement methods of the operation interface are carried out. Among them, force feedback is noticed as a technique to directly present contact force with the outside which is important in excavation work which is the main application of hydraulic excavators. However, the force characteristics perceived by a human when operating these levers are unknown. It is unclear whether the reaction force characteristics of the conventional lever without active force feedback and devices that present the machine's physical

3

information in terms of sense of force are optimal for humans. We clarify human force perception characteristics in lever operation and propose a lever force feedback design based on it.

1.2 Related Work

1.2.1 Operation Training Simulators of Hydraulic Excavator

Simulators can be effective for training in situations wherein it is difficult to train using an actual machine in a real environment. Training can be performed safely by using a simulator and with lower operating cost than that incurred when using the actual machine. Various studies have dealt with training using simulators, and several training simulators have been developed for construction machinery [1–3]. Some studies have considered the dynamics of the hydraulic excavator in simulators [4–6]. There exists a challenge in the case of excavator simulators: It is difficult to reproduce the behavior of soil excavated in real time because of the calculation cost. We think that this problem can be solved by using a training system using an RC toy excavator.

1.2.2 Quantitative Evaluation of Operation Skill of Hydraulic Excavator

Quantitative evaluation of operation skills is useful for training. Typically, the time spent on a work is used to evaluate the operating skills of hydraulic excavators, but this parameter is not sufficient for detailed skill evaluation. Research has been conducted on quantifying the operation skills of an excavator [7–9]. It is unknown, however, whether the skill evaluation method applied

for a real excavator can be applied when using an RC toy excavator that cannot completely simulate the characteristics of actual excavators. Therefore, it is necessary to verify the indices that can quantitatively evaluate the operation skill regardless of whether the operation target is a real excavator or an RC toy excavator.

1.2.3 Cockpit View Presentation by Virtual Reality in Teleoperation Systems and Training Systems

In order to increase the presence in a teleoperation system, a method of presenting images captured by a camera placed on the operation target to the user via a head mounted display (HMD) is adopted. For example, HMD-based mixed reality is used to enhance telepresence during the teleoperation of road vehicles and UAVs [10, 11]. It is also used for a teleoperated excavator [12]. The same method is also used for training systems using alternative machines such as RC toys and smaller machines. An operation training system using an RC helicopter has been developed [13]. This system provides a viewpoint from a cockpit in the helicopter by projecting images from a camera attached to the RC helicopter on an HMD and thus helps improve the reality of the operation. Override Ship Maneuvering Simulator is an actual training ship, and augmented reality (AR) technology has been developed [14]. This system gives the sensation of being on a large ship by displaying a three-dimensional (3D) model of a large ship superimposed on the HMD image using an AR marker installed at the bow. In this study, this technique is used to reproduce the field of view as if riding an RC toy excavator.

1.2.4 Feedback Design of the Operational Interface to Improve the Operability

It is essential to improve the excavator's operability. The feedback design of the operational interface of a tool or machine is directly linked to its operability. Conventional studies have shown that appropriate feedback design using graphics, sound, and vibration improves operability [15–17]. Ito *et al.* upgraded the operability of a teleoperated excavator by presenting the machine instability during excavation with visual information [18, 19]. The reaction force design of the operator interface also increases operability. Various studies have been conducted on force feedback devices to improve the operability of construction machinery by compensating for the lack of information when operating the excavator [20–22]. Some recent studies have logically dealt with the force feedback control to present stable forces under the influence of external factors [23–25]. However, the force characteristics a human perceives when operating these levers are unknown. It is unclear whether the reaction force characteristics of the conventional lever without active force feedback and devices that present the machine's physical information in terms of force sensors are optimal for humans. Therefore, we clarify human force perception characteristics in lever operation and propose a lever force feedback design based on it.

1.2.5 Perceived Force Characteristics by Human

The operability of a vehicle's steering wheel changes when the reaction force characteristics vary. Takemura *et al.* reported that the subjective perceptual force obtained by psychophysical experiments correlated more with the steering wheel operability than the quantitative physical force measured by

sensors [26]. Jones reported that the perceived force is affected by the physical characteristics of an object and the human psychophysical characteristics [27]. Furthermore, Takemura *et al.* reported that the perceptual force bias was affected by differences in posture while steering a vehicle [28]. McCloskey *et al.* revealed that the magnitude of effort is strongly correlated with the judgment of force and heaviness [29]. Cafarelli and Bigland-Ritchie discovered that the muscle activity could be used to estimate the effort [30]. Morree *et al.* provided neurophysiological evidence of the correlation between muscle activity and effort sensing [31]. These studies propose that the sense of effort can be predicted by estimating the muscle activity intensity. Kishishita *et al.* constructed a perceived force prediction model for steering operations by estimating the muscle activity based on posture, external force, and a three-dimensional (3D) musculoskeletal model [32]. They also explained the postural bias in the perception of the steering reaction force [33]. Thus, these previous studies advocate that the appropriate design of the perceived force can also enhance the operability of operational interfaces other than the steering wheel. Therefore, we tried to estimate the perceived force during lever operation by the same method and apply it to lever reaction force design.

1.3 Content Outline

The thesis is organized as follows:

In Chapter 2, the operation training system for a hydraulic excavator is described. We developed a training system by using an RC toy excavator with the same viewpoint and operating interface as a real excavator. Next, the dynamic characteristics, operability, and visual presence of the proposed system are verified.

In Chapter 3, the quantitative evaluation of operation skills that is essential in operation training is described. We verified indices that can quantitatively evaluate the operation skill of a real excavator using the proposed training system using the RC toy excavator. The results suggest that the operating skill of a real excavator can be partially evaluated by using the proposed system.

In Chapter 4, the force feedback design of operation levers considering the characteristics of human force perception to improve hydraulic excavator operability is described. We constructed a perceived force estimation model in the lever operation and evaluated the estimation accuracy. Next, we designed the lever reaction force considering the force perception characteristics using the proposed model and evaluated the operability of the designed lever. The operation skill evaluation indices examined in Chapter 3 and subjective evaluation indices on the operability are used to evaluate the operability. The results suggest that the operability of the excavator is improved by the lever reaction force design considering human force perception characteristics.

Finally, Chapter 5 concludes the dissertation and outlines the limitations and future work.

Chapter 2

Development of the Operation Training System for Hydraulic Excavator

2.1 Introduction

In Chapter 2, we describe the development of an operation training system for hydraulic excavators. Operation training with a real excavator may be difficult due to cost and safety issues. Simulators can be effective for training in situations wherein it is difficult to train using an actual machine in a real environment. Training can be performed safely by using a simulator and with lower operating cost than that incurred when using the actual machine. However, there exists a challenge in the case of excavator simulators: It is difficult to reproduce the behavior of soil excavated in real time because of the calculation cost. We think that this problem can be solved by using a training system using an RC toy excavator. In this study, we developed a simulator that can measure each joint angle in real time by using an RC toy excavator with the same viewpoint and operating interface as a real excavator.

The rest of the Chapter is organized as follows. Section 2.2 describes an operation training system developed using an RC toy excavator and VR tech-
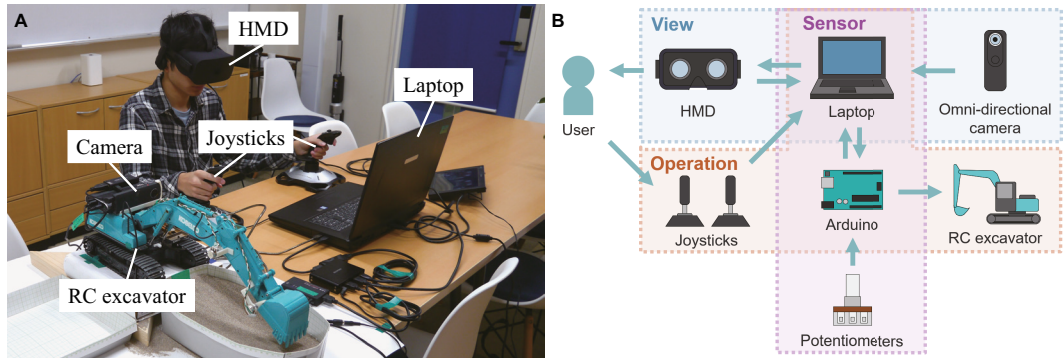
Fig. 2.1: System using RC toy excavator and VR technology. (A) System appearance and (B) System configuration. Written informed consent was obtained from the individual for the publication of this image.

nology. Section 2.3 describes the measurement of dynamic characteristics of the developed system. Section 2.4 describes the subjective evaluation of the operability and visual presence of the developed system. In Section 2.5, we discuss each result. Finally, Section 2.6 presents our conclusions and future work.

2.2 Operation Training System using an Remote Controlled Toy Excavator and Virtual Reality

Fig. 2.1 shows the overview and configuration of the developed system using an RC toy excavator and VR technology. This system consists of an RC toy excavator, an omnidirectional camera (RICOH, RICOH THETA S), an HMD (Oculus VR, Oculus Rift CV 1), two joysticks (Logitech, Extreme 3D Pro), four variable resistors (Linkman, R1610N-QB1-B103), a microcomputer board (Arduino SRL, Arduino Uno; hereinafter, referred to as Arduino), and a laptop computer.
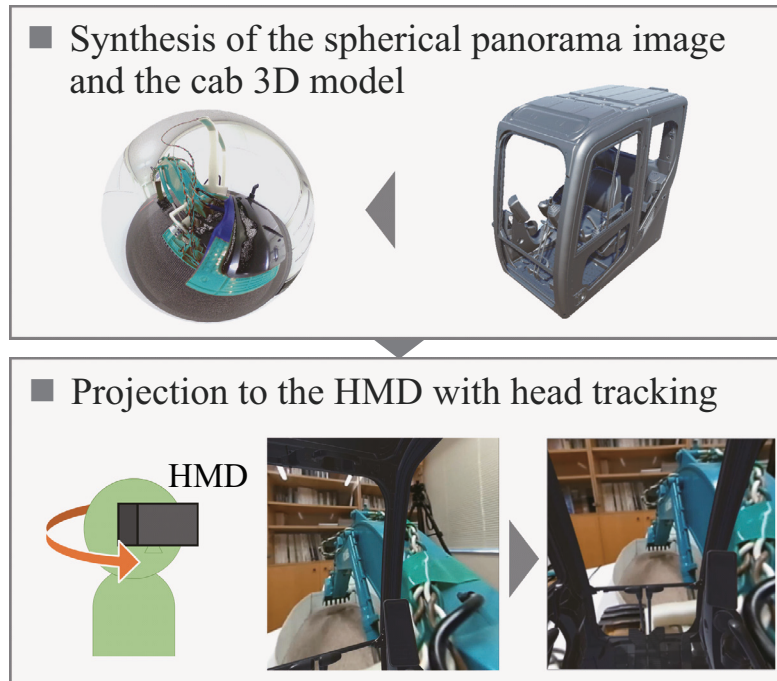
Fig. 2.2: Reproduction of field of view from cab.

The field of view from the cab of the excavator was reproduced in this system. Fig. 2.2 shows the method of reproducing the field of view from the cab. The omnidirectional camera was mounted on the RC toy excavator. The obtained images were transmitted to the laptop over HDMI, and spherical panoramic images were generated. A three-dimensional (3D) model of the cab of a hydraulic excavator was arranged at the center of the spherical panoramic image. The field of view from the 3D model of the cab was projected onto the HMD and it corresponded to the orientation of the user through the head-tracking function of the HMD. In this way, the user can experience a field of view as if he were on the RC toy excavator. A series of processing of image presentation was performed using the game engine Unity. The delay time of the visual system was about 170 ms. We modified the RC toy excavator so that it could be operated with the two joysticks. Thus, it was possible to perform
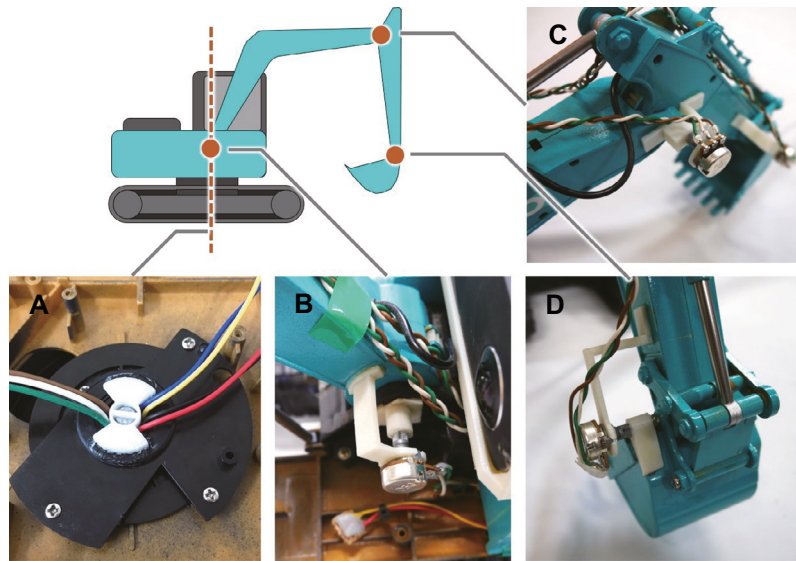
Fig. 2.3: Mounting position of each potentiometer. (A) Swing joint, (B) Boom joint, (C) Arm joint, and (D) Bucket joint.

the same operation as that for the real excavator. Moreover, it was possible to measure each joint angle of the RC toy excavator during the operation. As shown in Fig. 2.3, potentiometers were attached to the joints of the RC toy excavator. The control of the RC toy excavator and the measurement of the joint angles were realized by using the laptop and Arduino.

2.3 Measurement of Dynamic Characteristics of the Proposed System

2.3.1 Experimental Protocol

To confirm the dynamics of the RC toy excavator used in the proposed system, we measured the time response of each joint angular velocity of the RC toy excavator and real excavator (SK135SR-5, Kobelco Construction Machinery) shown in Fig. 2.4. Fig. 2.5 and Table 2.1 present the initial joint angles.

Fig. 2.4: Real excavator (SK135SR-5, Kobelco Construction Machinery).
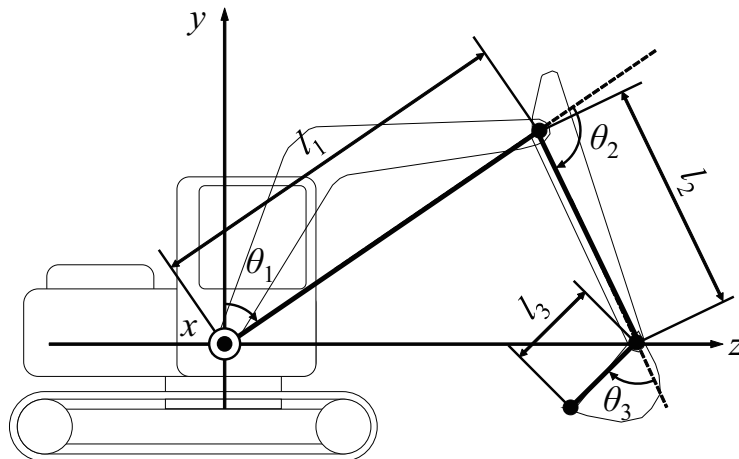
Fig. 2.5: Excavator geometry. l_1, l_2, and l_3 are the lengths of the boom, arm, and bucket, respectively. θ_1, θ_2, and θ_3 are the angles of the boom, arm, and bucket, respectively.

The lever operation performed manually for the real excavator was used as the input to the RC toy excavator.

Table 2.1: Initial joint angles of the excavator (°).

Operating target	θ_1	θ_2	θ_3
Boom	45	45	0
Arm	30	60	0
Bucket	30	45	45

2.3.2 Result

Fig. 2.6 shows the results of the time response of joint angular velocity. The blue dashed lines represent the lever operation normalized so that the maximum value becomes 1. The cyan and red solid lines represent the joint angular velocity of the real excavator and the RC toy excavator, respectively.

We assumed the system as a first-order system with a dead time and estimated the system parameters. The gain K was the final value of the angular velocity, and the dead time L and the time constant T were calculated by the following formulas.

$$L = t_p - \frac{v_p}{R}. \tag{1}$$

$$T = t_q - L. \tag{2}$$

Here, $(t_p; v_p)$ is the inflection point of the joint angular velocity during the acceleration. R is the slope at the inflection point. Further, t_q is the time when the angular velocity reaches 63.2 % of the final value, and t_p and t_q are the times based on the time when the lever input starts.

Table 2.2 lists the calculated system parameters of each link of the real excavator and the RC toy excavator, respectively.
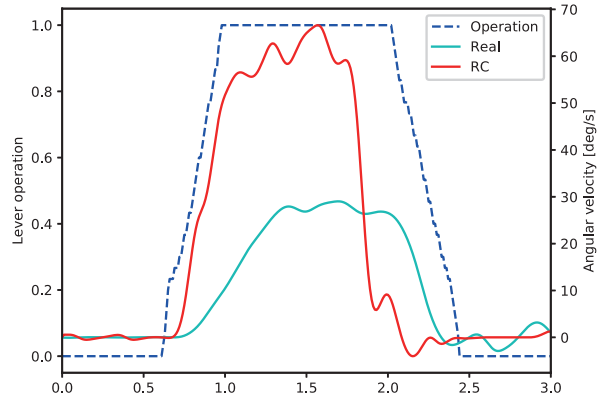
(a) Boom operation
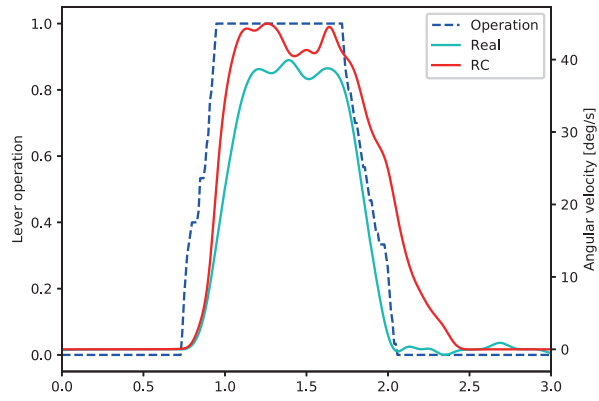
(b) Arm operation
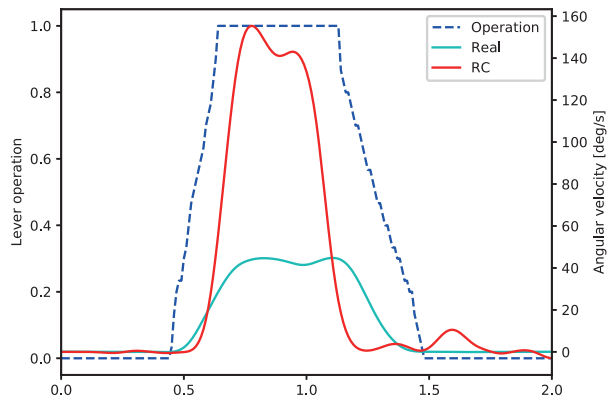
(c) Bucket operation

Fig. 2.6: Joint angular velocities of the real excavator and the RC toy excavator.

Table 2.2: System parameters of each link of excavator.

Type	Operating target	K	T	L
	Boom	29	0.31	0.22
Real excavator	Arm	39	0.16	0.12
	Bucket	43	0.12	0.07
	Boom	63	0.21	0.11
RC toy excavator	Arm	43	0.10	0.12
	Bucket	143	0.09	0.15

2.4 Subjective Evaluation of the Operability and Presence of the Proposed System

2.4.1 Experimental Protocol

The subjects were 8 individuals who had operated an excavator and 12 individuals who had never operated one; informed consent was obtained from the subjects before the experiment. The subjects performed repeated continuous excavation for 3 min. Continuous excavation consisted of four steps: excavating, turning, dumping, and returning. Moreover, continuous excavation began with the extension of the arm of the excavator, and the excavation was performed by digging into the ground. Turning was performed by turning the excavator by 90° while raising its bucket. Dumping was performed by discharging the soil into the bucket. Returning was defined as the operation of returning to the initial state of the excavation. After completing the task, we conducted a subjective evaluation of the operability of this system and the presence of the images by using a questionnaire. The operability was evaluated using six scales of the Japanese version of NASA-TLX [34], which is a subjective evaluation method for a mental workload. The overall workload was calculated using Raw TLX, which uses the average value of all scales.

The presence of the images was evaluated using four scales by referring to an evaluation questionnaire for the presence of a wide-field still image [35]. The questionnaire items are shown below.

- Operability

  - How much mental and perceptual activity was required?

  - How much physical activity was required?

  - How much time pressure did you feel due to the pace at which the tasks or task elements occurred?

  - How successful were you in performing the task?

  - How hard did you have to work to accomplish your level of performance?

  - How irritated, stressed, and annoyed versus content, relaxed, and complacent did you feel during the task?

- Presence of the images

  - How much do you feel the presence?

  - How much did you feel the powerfulness?

  - How much did you feel the comfort?

  - How much did you feel the depth?

Each item was answered with 0 to 100 points.

2.4.2 Result

Fig. 2.7(a) shows the questionnaire results of the subjective evaluation of operability. This radar chart means that the larger the area, the greater is the
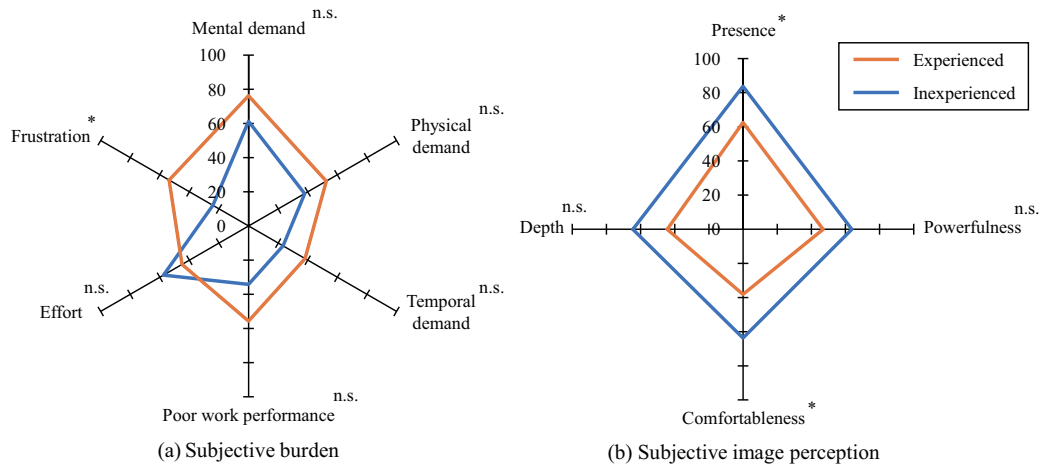
Fig. 2.7: Assessment results for subjective burden and image perception (*: $p < 0.05$, n.s.: not significant).

operational burden. As seen from the graph, the experienced subjects tended to give higher scores than the inexperienced ones for the items other than "effort." The t-tests between the experienced and inexperienced subjects for each item shows that there is no significant difference in "mental demand," "physical demand," "temporal demand," "poor work performance," and "effort," but a significant difference was confirmed for the item "frustration." Fig. 2.8 shows the overall workload by Raw TLX. This result confirms that the experienced subjects find operating the RC toy excavator more difficult. Fig. 2.7(b) shows the questionnaire result of the subjective evaluation of the presence of the images. This radar chart shows that the larger the area, the better is the presence of the images. The graph shows that the experienced subjects tend to give lower scores than the inexperienced subjects for all items. The t-tests between the experienced and inexperienced subjects for each item show that there is no significant difference in terms of "powerfulness" and "depth," but there is a significant difference in the case of "presence" and "comfortable-
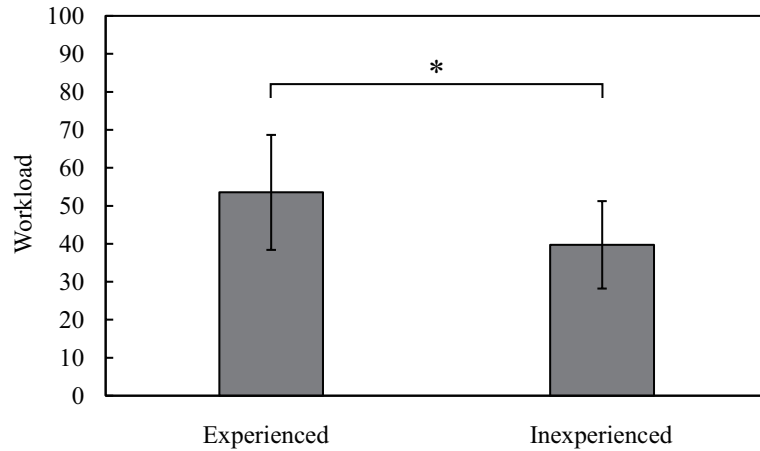
Fig. 2.8: Results of overall workload (Raw TLX, *: $p < 0.05$).

ness." This result confirms that the experienced subjects tend to give lower scores for presence and comfort.

2.5 Discussion

Fig. 2.7(a) and Fig. 2.8 indicate that the experienced operators find it more difficult to operate the RC toy excavator. Fig. 2.7(b) indicates that the experienced operators tend to give lower scores for presence and comfort. The reason for this may be that the experienced operators felt a sense of incongruity in the RC toy excavator that differs in operability and visibility from real excavators. Actually, the dynamic characteristics of the proposed system were greatly different from those of the real excavator as shown in Fig. 2.6 and Table 2.2. The operation interface was reproduced with the gaming joysticks that have different stiffness from the real lever. Therefore, the operability of the RC toy excavator was not exactly the same as that of the real excavator. Moreover, we replaced the original human vision by the HMD and omnidirectional camera with much lower resolution than the human eye. The current system was not

capable of providing depth information. Nevertheless, the evaluation of depth perception was not much worse because the depth was perceived in a monocular image with the help of environmental conditions such as lighting, shadows, etc. In addition, the latency of the visual system has a great influence on visual immersion. In order to enable more effective training, it is necessary to closely reproduce the operability and visibility of real excavators in the RC toy excavator.

The importance of sense of embodiment (SoE) and embodiment of cognition (EoC) in a VR environment [36, 37] was emphasized. Improving SoE and EoC will extend the completeness of the operation training. Multimodal information such as vision, hearing, and haptic sensations can be also used for gaining a better understanding of more advanced skills when operating real excavators. Multimodal information is very important for enhancing EoC and SoE. As future work, we plan to improve the proposed system to display sounds and vibrations during operations.

2.6 Conclusion

In this section, we developed the operation training system using an RC toy excavator and VR technology with the same viewpoint and operating interface as a real excavator. We investigated the dynamic characteristics of the RC toy excavator used in the developed system. The results showed that the dynamic characteristics of the RC toy excavator are significantly different from those of the real excavator. Next, we evaluated the operability and presence of the developed system by questionnaire. The results indicate that the experienced operators find it more difficult to operate the RC toy excavator and tend to give lower scores for presence and comfort. The reason for these results may

be that the experienced operators felt a sense of incongruity in the RC toy excavator that differs in operability and visibility from real excavators.

In the future, in order to enable more effective training, we will attempt to closely reproduce the operability and visibility of a real excavator in the RC toy excavator. Specifically, we will adopt the control of the motor in which the dynamic characteristics of the RC toy excavator become equal to those of the real excavator. And also, we will replace the joysticks with the same levers as those of the real excavator and improve the visual system using an industrial camera with high resolution and low delay.

Chapter 3

Verification of Operation Skill Evaluation Indices of Excavator

3.1 Introduction

In Chapter 3, we describe the quantitative evaluation of operation skills that is essential in operation training. In general, the time spent on work is used to evaluate the skills required to operate a hydraulic excavator, but this index is not sufficient for detailed skill evaluation. Therefore, various studies have been conducted on the quantitative evaluation of operation skills of excavators. However, it is unclear whether the skill evaluation indices used in the real excavator can be applied when using the RC toy excavator that does not completely reproduce the characteristics of the real excavator. We verified indices that can quantitatively evaluate the operation skill of a real excavator using the RC toy excavator.

The rest of the Chapter is organized as follows. Section 3.2 describes the calculation method of operation skill evaluation indices. Section 3.3 explains skill evaluation of excavation operation using the RC toy excavator and the

real excavator. In Section 3.4, we discuss the results of the skill evaluation. Finally, Section 3.5 presents our conclusions and future work.

3.2 Calculation Method of Operation Skill Evaluation Indices

The evaluation indices were the operation time t, dispersion of bucket trajectories d_t, length of bucket trajectory l, average bucket velocity $\bar{v}$, and dispersion of lever operations d_o. Each index was calculated for one cycle of the continuous excavation, excavating section, turning section, dumping section, and returning section.

The operation time was calculated because it is typically used as an evaluation index. The dispersion of the bucket trajectory and the dispersion of the lever operation were calculated based on the fact that experts excavate with an approximately unique trajectory, regardless of the excavation order [8]. The trajectory length of the bucket was calculated by considering that the experts had shorter trajectories with more compact operation. The average bucket velocity was calculated by considering that experts performed faster operations. Each index was calculated using the methods described below.

The dispersion of the bucket trajectories represents the degree of difference among the trajectories, when the same operation was performed multiple times. Fig. 3.1 shows the calculated dispersion flow for the bucket trajectories. First, the average of these trajectories was calculated. However, it was impossible to calculate the average trajectory because the data length was different for each trajectory. Therefore, the average of the trajectories with different data lengths was calculated using the DTW barycenter averaging (DBA) method [38]. Then, the dissimilarity between each trajectory and the
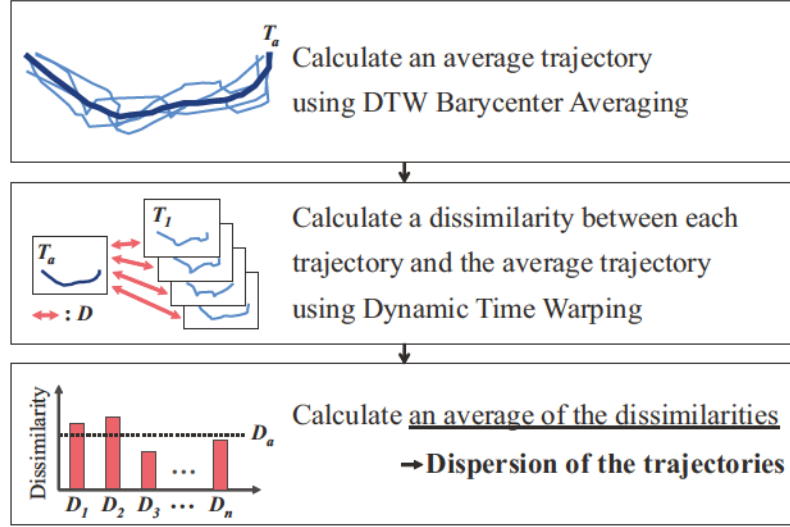
Fig. 3.1: Method of calculating dispersion trajectories.

average trajectory was calculated. For this purpose, the dynamic time warping (DTW) method [39], which can calculate the dissimilarity between two time series with different lengths, was adopted. Finally, the average dissimilarity was calculated, and this was considered as the dispersion of the trajectories d.

The bucket trajectory length l was calculated using the following equation:

$$l = \sum_{i=1}^{n-1} \sqrt{(x_{i+1} - x_i)^2 + (y_{i+1} - y_i)^2 + (z_{i+1} - z_i)^2}. \tag{3}$$

Here, (x_i, y_i, z_i) is the i-th coordinate of the bucket trajectory with n elements.

The average velocity of the bucket $\overline{v}$ was calculated as follows:

$$\overline{v} = \frac{l}{t}. \tag{4}$$

The dispersion of the lever operations d_o was calculated in the same manner as d_t for the swing operation, boom operation, arm operation, and bucket operation. Here, the distance function $d(a_i, b_j)$ of the lever operation is defined as follows:

24

$$d(a_i, b_j) = |a_i - b_j|. \tag{5}$$

3.3 Operation Skill Evaluation of Excavation Performed by the Toy Excavator and Real Excavator

3.3.1 Experimental Protocol

The RC toy excavator and real excavator (SK135SR-5, Kobelco Construction Machinery) considered in this study are shown in Fig. 2.1 and Fig. 2.4, respectively. The subjects were three expert and five non-expert operators. Informed consent was obtained from them before the experiment. In this study, an operator who typically evaluates the operability of a hydraulic excavator was considered as an expert. The subjects performed the following task five times after sufficient practice using the RC toy excavator and real excavator. The measurement task consisted of three continuous excavation cycles. The second and third cycles were analyzed, and the first cycle starting from the stopped state was excluded. The operation time, operation amount of each lever axis, and each joint angle of the excavator were measured. The angle of the boom, arm, and bucket of the real excavator were calculated from the measured length of the hydraulic cylinder of the excavator, and the swing angle was measured using an angular acceleration sensor. The pilot pressure of each lever of the actual excavator was used as the operation amount of each lever axis. For the RC toy excavator, the sampling rate of the measurement data was 100 Hz. For the real excavator, the sampling rate of the measurement data was 1,000 Hz, and this was reduced to 100 Hz. The 3D trajectory of the

bucket tip was calculated from the joint angle of the excavator by calculating the forward kinematics as follows:

$$
\begin{bmatrix} x \\ y \\ z \end{bmatrix} = \begin{bmatrix} (l_1 s_1 + l_2 s_{12} + l_3 s_{123}) s_4 \\ l_1 c_1 + l_2 c_{12} + l_3 c_{123} \\ (l_1 s_1 + l_2 s_{12} + l_3 s_{123}) c_4 \end{bmatrix}. \tag{6}
$$

$$
\begin{cases}
s_i & = \sin\theta_i, \ i = 1, 4 \\
c_i & = \cos\theta_i, \ i = 1, 4 \\
s_{12} & = \sin(\theta_1 + \theta_2) \\
c_{12} & = \cos(\theta_1 + \theta_2) \\
s_{123} & = \sin(\theta_1 + \theta_2 + \theta_3) \\
c_{123} & = \cos(\theta_1 + \theta_2 + \theta_3)
\end{cases} \tag{7}
$$

Here, the rightward, upward, and forward directions of the excavator were set as the positive directions of the x, y, and z axes, respectively, as shown in Fig. 2.5. Here, l_1 is the length of the line segment connecting the rotation axis of the boom and the arm's rotation axis; l_2 is the length of the line segment connecting the rotation axis of the arm to the rotation axis of the bucket; l_3 is the length of the line segment connecting the rotation axis of the bucket to the bucket tip; θ_1 is the angle between the line segment l_1 and the vertical direction; θ_2 is the angle between the line segment l_1 and segment l_2; θ_3 is the angle between the line segment l_2 and line segment l_3; and θ_4 is the angle of the upper revolving body with respect to the lower traveling body. The parameters of the real excavator and the RC toy excavator as listed in Table 3.1 were used to calculate the trajectory.

3.3.2 Result

Fig. 3.2 shows examples of the measurement trajectory, and the lever operation during one excavation cycle with the RC toy excavator and real excavator.

Table 3.1:   Length of each link (mm) and movable range of each joint (°) of excavator.

Type	l_1	l_2	l_3	θ_1	θ_2	θ_3
Real excavator	5,650	2,940	1,440	28–137	30–159	-41–142
RC toy excavator	255	125	90	30–100	44–115	0–90

(a) Trajectory of RC excavator bucket (mm)

(b) Lever operation of RC excavator

(c) Trajectory of real excavator bucket (mm)

(d) Lever operation of real excavator
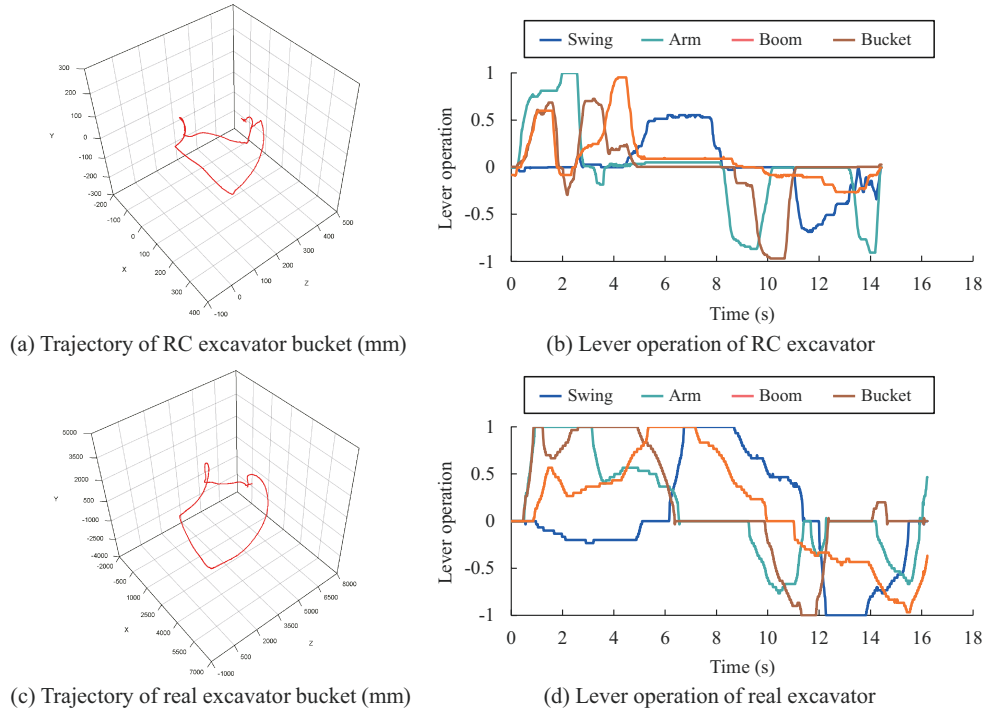
Fig. 3.2:   Measurement data during excavation (Expert 1, Task 3, Cycle 1).

Here, the lever operation is represented by the time series of the value obtained by normalizing the inclination degree of the turning, boom, arm, and bucket operation levers, from -1 to 1. It was assumed that the excavators differed in terms of the trajectory shape and waveform of the lever operation amount owing to the difference in the ratio of the length of the links and the behavior of the excavator's behavior. These data were calculated using the operation skill evaluation indices.

1. Operation time   2. Length of bucket trajectory
3. Average velocity of bucket
4. Dispersion of bucket trajectory
5-8. Dispersion of lever operation (swing, boom, arm, bucket)
— RC excavator   — Real excavator

(a) Expert 1

(b) Expert 2

(c) Expert 3

(d) Non-expert 1

(e) Non-expert 2

(f) Non-expert 3

(g) Non-expert 4

(h) Non-expert 5
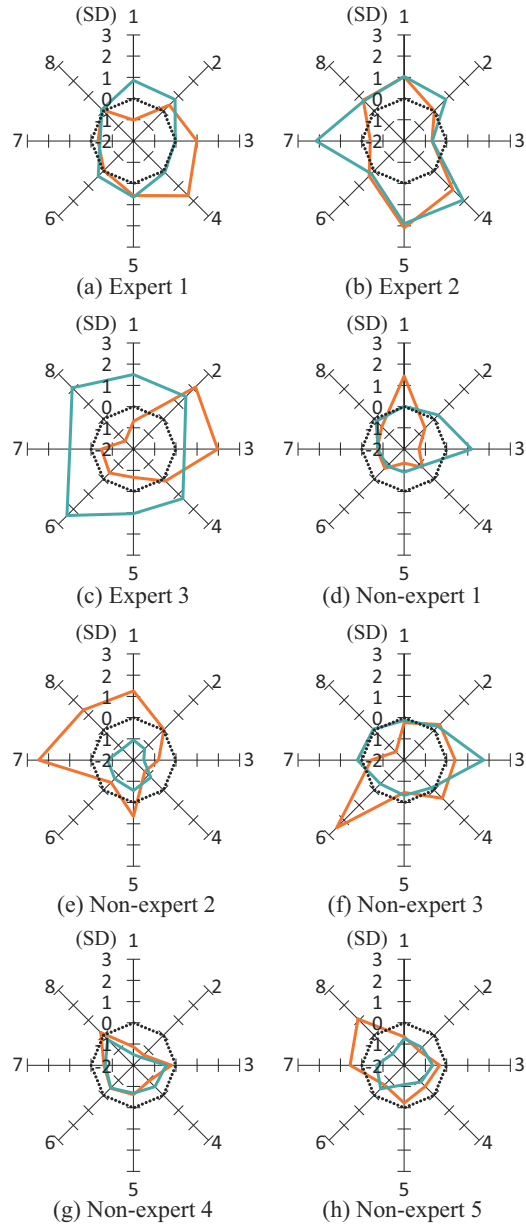
Fig. 3.3:   Radar chart of evaluation indices. The standardized reciprocal of each evaluation index was used such that the area of the radar chart became larger for a highly-skilled subject. The dotted line represents the average for all the subjects.

Fig. 3.3 shows the evaluation indices of the RC toy excavator and the real excavator on the radar chart for each subject. The first axis represents the operation time; the second axis represents the length of the bucket trajectory; the third axis represents the average velocity of the bucket; the fourth axis represents the dispersion of the bucket trajectory; and the fifth to eighth axes represent the dispersion of the lever operation for the swing, boom, arm, and bucket. The standardized reciprocal of each evaluation index was used such that the area of the radar chart was greater for a highly-skilled subject. The dotted line represents the average for all subjects. The figure shows that the average is better than the average in the case that the evaluation index is outside this line. It was confirmed that the experts tended to have a larger radar chart area than the nonexperts for both the RC toy excavator and the real excavator. The radar chart area for non-expert 3 was larger than that for the other nonexperts, because non-expert 3 had more working experience on operating a hydraulic excavator than the other nonexperts. These results suggest that it is possible to distinguish the skill differences for an expert or non-expert and to distinguish the length of working experience of the hydraulic excavator operator by using the RC toy excavator. However, the outline of the radar chart of the RC toy excavator was different from that of the real excavator. This may have been caused by the fact that the behavior of the RC toy excavator considered in this study differed from that of the real excavator.

The correlation of each evaluation index between the RC toy excavator and the real excavator was investigated for each section of the continuous excavation. Table 3.2 lists the calculated result of the correlation between the real excavator and the RC toy excavator for all evaluation indices. Each row represents an evaluation index, while each column represents the section considered in the calculation. Each value represents the correlation coefficient between

29

Table 3.2: Correlation between real excavator index and RC toy excavator index (* : $p < 0.05$, ** : $p < 0.01$). t is the operation time. d_t is the dispersion of bucket trajectories. l is the length of bucket trajectory. $\bar{v}$ is the average bucket velocity. d_o is the dispersion of lever operations.

Index	One cycle	Excavating	Turning	Dumping	Returning
t	0.09	−0.10	0.08	−0.26	0.56
d_t	**0.80**	−0.04	**0.82**	****0.87**	0.31
l	**0.73**	0.06	**0.80**	0.35	**0.78**
$\bar{v}$	0.23	**0.76**	0.15	0.68	−0.36
d_o (swing)	0.51	−0.38	0.26	0.32	0.60
d_o (boom)	0.35	0.40	**0.80**	−0.01	−0.29
d_o (arm)	−0.33	−0.25	0.46	0.37	0.02
d_o (bucket)	−0.64	−0.60	0.02	0.63	−0.49

the real excavator and RC toy excavator for each evaluation index. The values with significant correlation are shown in boldface. No significant correlation between the real excavator and the RC toy excavator data was found in any section of the operation time and dispersion of the swing, arm, and bucket operations. However, in several sections, significant correlation was confirmed for the dispersion of the bucket trajectories, length of the bucket trajectory, average velocity of the bucket, and dispersion of the boom operations.

3.4 Discussion

Table 3.2 lists the calculated result of the correlation between the real excavator and the RC toy excavator for all evaluation indices. It was thought that the correlation of the dispersion of the bucket trajectories and length of the bucket trajectory is higher because it was unaffected by the difference in the behavior of the excavator. The results suggest that it is possible to partly evaluate the operation characteristics of a real excavator by using an RC toy excavator whose dynamics differed from those of a real excavator.

However, significant correlations could not be confirmed between the RC toy excavator and real excavator on the other indices. The reason for this may be that the RC toy excavator differs in operability and visibility from real excavators as described in Chapter 2. In order to enable more detailed skill evaluation, it is necessary to closely reproduce the operability and visibility of real excavators in the RC toy excavator.

3.5 Conclusion

In this section, we verified indices that can quantitatively evaluate the operation skill of a real excavator using the RC toy excavator. We calculated evaluation indices for lever operation and bucket movement during excavation using the proposed system and a real excavator. Although the dynamics were largely different, the results showed a high correlation between the RC toy excavator and real excavator in some operations and suggested that the proposed system could evaluate the operational skills with regard to the correspondence between the direction of the lever and the joint angle of the excavator.

However, not all the operation skills of the real excavator can be learned by training with the RC toy excavator system developed in this paper. In the future, in order to enable more accurate skill evaluation, we will attempt to closely reproduce the operability and visibility of a real excavator in the RC toy excavator. Specifically, we will adopt the control of the motor in which the dynamic characteristics of the RC toy excavator become equal to those of the real excavator. And also, we will replace the joysticks with the same levers as those of the real excavator and improve the visual system using an industrial camera with high resolution and low delay. This study is limited to the evaluation of the operation skills of hydraulic excavators using the RC toy

excavator, and it has not been verified whether effective training can actually be performed using it. Therefore, we plan to verify the training effect of the RC toy excavator by observing the changes in the operation skills over time with such training.

Chapter 4

Force Feedback Design of Operation Levers Considering the Characteristics of Human Force Perception to Improve Hydraulic Excavator Operability

4.1 Introduction

In Chapter 4, we describe the force feedback design of operation levers considering the characteristics of human force perception to improve hydraulic excavator operability. Various researches on the feedback of the machine information as one of the improvement methods of the operation interface have been carried out. Among them, force feedback is noticed as a technique to directly present contact force with the outside which is important in excavation work which is the main application of hydraulic excavators. However, the force characteristics a human perceives when operating these levers are unknown. It is unclear whether the reaction force characteristics of the conventional lever without active force feedback and devices that present the machine's physical information in terms of force sensors are optimal for humans. We proposed a

perceived force prediction method for the lever operation based on a musculoskeletal simulation. Moreover, we developed the lever such that the perceived force varied linearly with the lever angle and verified the effect of the proposed lever reaction force on the operability when performing the leveling task with the excavator.

The rest of the Chapter is organized as follows. Section 4.2 describes the construction of a perceived force prediction model for the lever operation. Section 4.3 describes the verification of of lever reaction force design considering force perception character. Section 4.4 discusses the results. Finally, Section 4.5 presents our conclusions and future work.

4.2 Construction of Perceived Force Prediction Model during Lever Operation

4.2.1 Methodology

In this study, a perceived force prediction model was constructed for the lever operation following the perceived force prediction method for the steering operation of a car, as proposed by Kishishita *et al.* [32]. Their estimation method is explained below. The perceived force when a reaction force is applied while holding the steering wheel is measured. The relationship between the applied force F_a and the perceived force F_p follows the Weber–Fechner law [40] and is approximated by the following equation:

$$F_p = a_0 \log F_a + b_0, \tag{8}$$

where a_0 and b_0 are coefficients when the steering angle is 0°. Here, the force perception-change ratio P is defined as follows:

$$P = \frac{F_p}{F_a} = \frac{a_0 \log F_a + b_0}{F_a}. \tag{9}$$

Here, P is determined uniquely using F_a. However, Takemura et $al.$ reported that the perceived force changes depending on the body posture [28]. As described in the Introduction, a human judges the force based on the sense of effort [29]. The applied muscle varies according to posture, even when the hand outputs the force in the same direction and with identical magnitudes. Therefore, the sense of effort also changes when the posture varies. Cafarelli and Bigland-Ritchie revealed that the muscle activity could be used to estimate the effort [30]. This fact suggests that describing the change in the perceived force depending on the posture can be actualized by expressing the force perception-change ratio using the muscle activity instead of the applied force. Kishishita et $al.$ explained the force perception-change ratio using the muscle activity estimated by a 3D musculoskeletal simulation. They confirmed the linear relationship between the applied force F_a and muscle activity α in the steering posture. α is expressed by the following equation:

$$\alpha = k_j F_a + m_j, \tag{10}$$

where k_j and m_j are coefficients when the steering angle is j. (10) expresses the relationship between F_a and α when the reaction force is applied while the steering angle is maintained at j. k_j and m_j are determined according to the posture in which the muscle activity is estimated because they change depending on the steering angle j. Furthermore, (10) shows that the postural effect on the muscle activity varies according to the steering angle and correlates with the human sense of force. The following equation is obtained by rearranging (10):

$$F_a = \frac{\alpha - m_j}{k_j}. \tag{11}$$

Then, the following equation is obtained by substituting (11) into (9):

$$P = \frac{F_p}{F_a} = \frac{k_j \left(a_0 \log\left(\frac{\alpha - m_j}{k_j}\right) + b_0\right)}{\alpha - m_j}. \tag{12}$$

This equation demonstrates that the force perception-change ratio can be expressed as a function of the muscle activity based on the posture when the steering angle is j. The muscle activity can be obtained via optimization calculations using a musculoskeletal model with the posture and external force as inputs. Thus, P for a particular posture can be computed from the representative value of α. Finally, F_p is given as a function of F_a by the following equation:

$$F_p = P \cdot F_a. \tag{13}$$

In this study, we constructed a perceived force prediction model for the lever following the above method. However, it was unconfirmed whether (8) and (10) are satisfied during the lever operation. Therefore, we investigated the perceived force and muscle activity characteristics for the applied force during the lever operation.

4.2.2 Muscle Activity Estimation Method by Musculoskeletal Simulation

In this study, we estimated the muscle activity using OpenSim, an open-source software for biomechanical modeling, simulation, and analysis [41]. The 3D musculoskeletal model was developed based on the previously reported body

model [42]. Moreover, the muscle force was calculated using the muscle contraction model based on the Hill-type muscle model with elastic and contractile components proposed by Thelen [43]. The maximum isometric force F^M, optimal muscle-fiber length l^M, and pennation angle of the muscles were determined based on the parameters reported by Holzbaur *et al.* [44]. The muscle activity was obtained from the motion and external force data via optimization computations in OpenSim. First, the joint angle and torque were estimated by inverse kinematics and inverse dynamics calculations from the external force and marker position data measured using the motion capture system. Then, the muscle force that balances the joint torque was determined by optimizing the muscle activity. Here the muscle activity of the m-th muscle satisfies the following equation:

$$\sum_{m=1}^{n} (\alpha_m F_m^0) r_{m,j} = \tau_j, \tag{14}$$

where F_m^0 is the maximum isometric force, τ_j is the joint torque of the j-th joint, and $r_{m,j}$ is the moment arm parameter. α is a continuous variable bounded by $\alpha_m (0 \leq \alpha_m \leq 1)$; it can be viewed as the controls to the musculoskeletal system [41]. By using the relationship between the motor unit firing rate and muscle activity, the muscle activity (muscle excitation) is increased by increasing the motor unit firing rate [45]. The moment arm parameters were determined using the muscle length of the m-th muscle l_m and joint angle of the j-th joint θ_j [46, 47]:

$$r_{m,j} = \frac{dl_m}{d\theta_j}. \tag{15}$$

The relationship between the muscle force F_m and the muscle activity α_m are given as follows:

Fig. 4.1: Force presentation lever.

$$F_m = \alpha_m F_m^0 \overline{f}_l(\bar{l}_m) + F_m^0 \overline{F}^{PE}(\bar{l}_m), \tag{16}$$

where $\bar{l}_m$ is the normalized fiber length, $\overline{f}_l(\bar{l}_m)$ is the normalized active force–length relationship, and $\overline{F}^{PE}(\bar{l}_m)$ is the normalized passive force–length relationship; for this study, $\overline{f}_l(\bar{l}_m)$ and $\overline{F}^{PE}(\bar{l}_m)$ were obtained from a previous study [43].

4.2.3 Perceived Force Characteristics for Applied Force

When the applied force was applied in the posture of holding the lever at the neutral position, the perceived force was measured to investigate the perceived force characteristics for the applied force in the lever operation. Fig. 4.1 shows the force presentation lever used in the experiment. This equipment has three components: a commercially available force feedback steering controller (Thrustmaster, T500RS), a grip part of the lever of an excavator, and a 3D

(a) Displayed screen   (b) Experiment environment
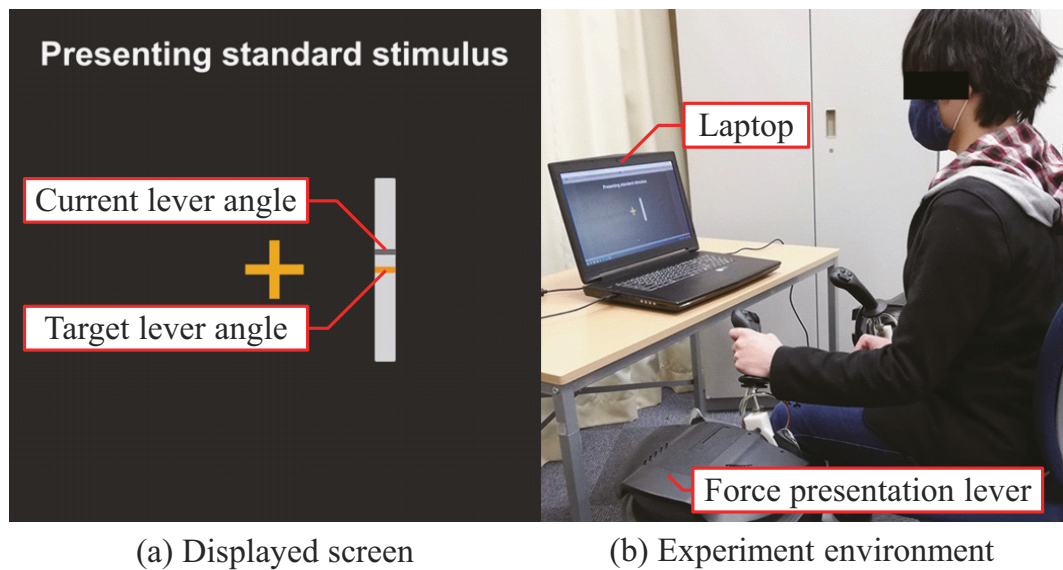
Fig. 4.2: Measurement experiment of perceived force characteristics for the applied force. The image shows the subject with force applied while looking at the lever angle gauge displayed on the laptop. Informed consent was obtained from the individual for publishing this image.

printed part for attaching the grip to the steering shaft. The operation direction was switched by rotating the mounting direction of the grip 90° and rotating the sitting orientation with respect to the equipment 90° in the opposite direction. The game engine Unity was used to control the equipment's applied force and perform the experiment. It was confirmed in advance that the equipment accurately outputs the force using the force sensor. Fig. 4.2 shows an image taken while measuring the perceived force characteristics for the applied force. The subjectively perceived force was measured using the magnitude estimation method [48]. The experimental procedure is as follows:

1. The subjects sit on the seat and hold the lever at the neutral position with their left hand. Afterward, a standard stimulus is given through the lever. The subjects hold the lever stationarily and memorize the

standard stimulus.

2. Next, a comparison stimulus is given through the lever. Subsequently, the subjects report the magnification of the comparison stimulus relative to the standard stimulus.

3. The standard stimulus is 9 N, and the comparison stimuli range from 6 to 13 N with a 1-N increment. The comparison stimuli are presented at random, and steps 1 and 2 are repeated until each comparison stimulus is presented five times.

The above experimental tasks were conducted in four directions following the operation directions of the lever: forward, backward, outward, and inward. The applied force was gradually increased for 4 s and afterward for 5 s more with a fixed force to avoid habituation error [49]. Three male subjects (average age: 22.7 ± 0.5 years) participated in the experiment. Informed consent was obtained from the subjects, and their health conditions were verbally enquired. The subjects practiced the experimental task for about 5 min before the experiment.

Fig. 4.3 shows the perceived force characteristics with respect to the applied force for each operating direction. Here, the applied force acts opposite to the operation direction. The error bar represents the standard deviation of the perceived force of all subjects, and the dotted line represents the approximate curve. These results show that the perceived force is proportional to the logarithm of the applied force. The characteristics shown in this figure indicate that the relationship between the applied and perceived forces follows the Weber–Fechner law [40] and that (8) is satisfied even in the lever operation. The slope a_0 and intercept b_0 of the following equation that replaced (8) were
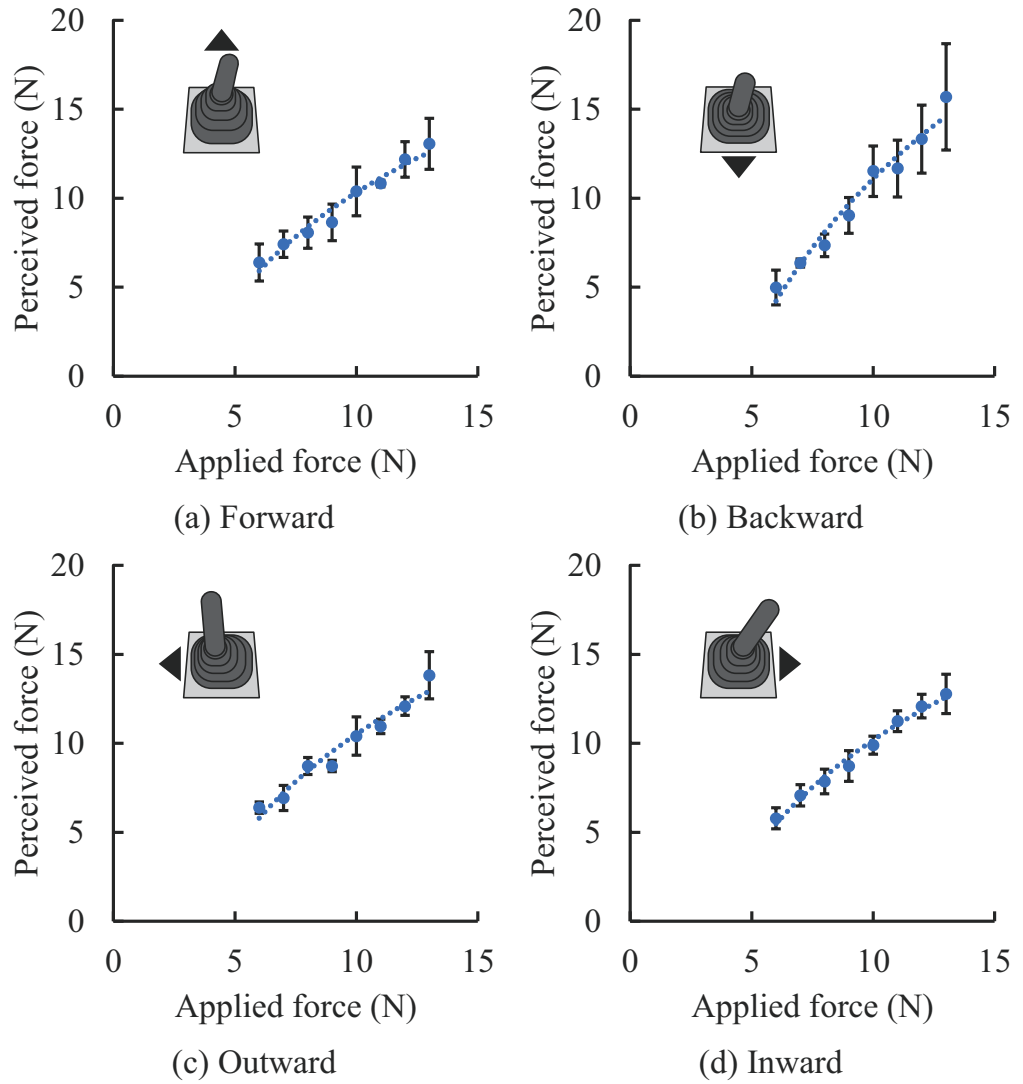
Fig. 4.3: Perceived force characteristics for the applied force in each postural direction when the lever angle is 0°.

calculated by the least-squares method from the measured perceived force for each applied force:

$$F_p = a_0 F_a' + b_0, \tag{17}$$

where

Table 4.1: Coefficients a_0 and b_0, and the coefficients of determination R^2.

Direction	a_0	b_0	R^2
Forward	8.63	-9.54	0.965
Backward	13.40	-19.90	0.964
Outward	9.13	-10.50	0.953
Inward	9.21	-11.00	0.985

$$F_a' = \log F_a. \tag{18}$$

The coefficient of determination R^2 was calculated employing the following equation:

$$R^2 = 1 - \frac{\sum_{i=1}^{n}(y_i - \hat{y}_i)^2}{\sum_{i=1}^{n}(y_i - \bar{y})^2}. \tag{19}$$

Here, y_i is the i-th measured value, $\bar{y}$ is the average value of the measured values, and $\hat{y}_i$ is the i-th calculated value using the regression equation. Table 4.1 lists the coefficients a_0 and b_0, and the coefficient of determination R^2.

4.2.4 Muscle Activity Characteristics for the Applied Force

When the force was applied in the posture of holding the lever at a certain angle, the muscle activity was estimated to investigate the muscle activity characteristics for the applied force during the lever operation. The muscle activity was estimated using OpenSim, an open-source software system for biomechanical modeling, simulation, and analysis [41]. Moreover, the stationary postures were obtained when holding the lever with the left hand at 0°–25° forward and backward and 0°–20° outward and inward with an interval of 2.5°. The postural data were obtained using seven motion capture cameras (Acuity
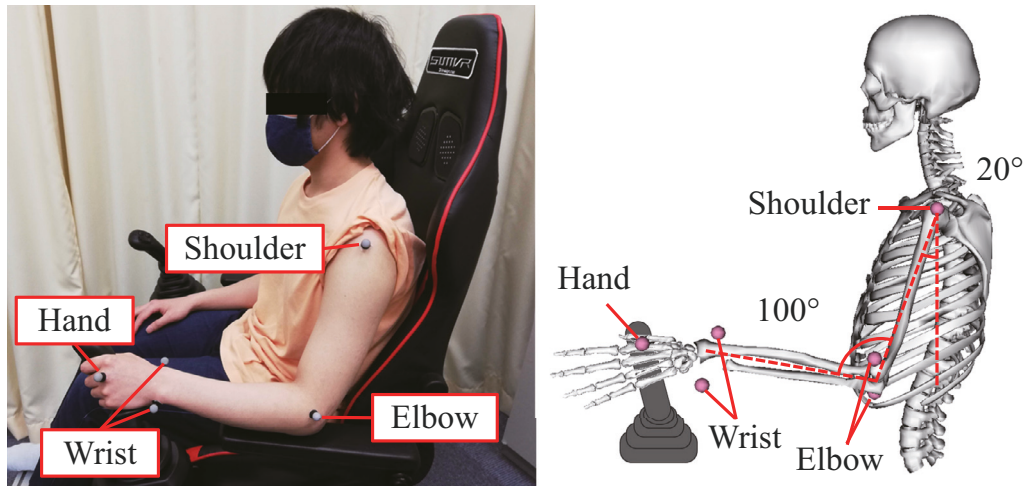
Fig. 4.4: Motion-capturing system and model postural conditions. Informed consent was obtained from the individual for publishing this image.

Inc., OptiTrack PrimeX 13 W) installed around the subject. Fig. 4.4 shows the posture when holding the lever at the neutral and mounting positions of the motion capture markers. A force ranging from 0 to 12 N with a 2-N interval was directly applied to the capitate bone at the wrist because the muscles from the wrist to the fingertip were not considered. Herein, the average muscle activity was defined for the following muscles, which were especially active for each operational direction.

- Forward direction: the anterior head of the deltoid (DELT1), medial head of the deltoid (DELT2), infraspinatus (INFSP), and long head of the biceps brachii (BIClong)

- Backward direction: the posterior head of the deltoid (DELT3), subscapularis (SUBSC), teres major (TMAJ), and long head of the triceps brachii (TRIlong)

- Outward direction: the posterior head of the deltoid (DELT3), supraspina-

43
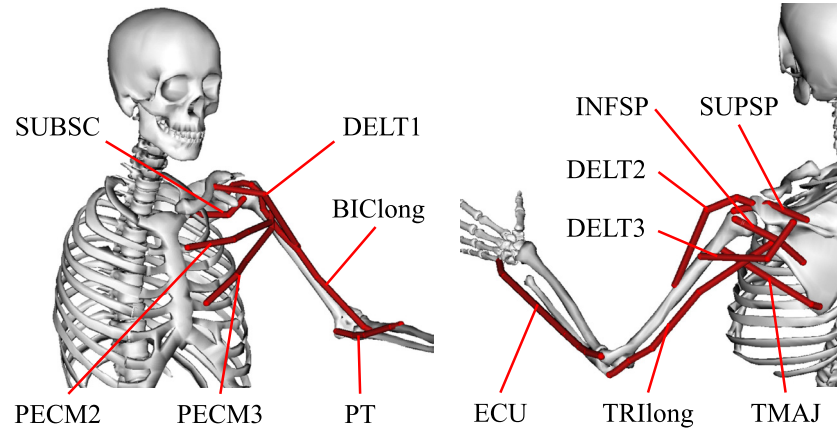
Fig. 4.5: Muscles applied to estimate muscle activity.

tus (SUPSP), infraspinatus (INFSP), long head of the triceps brachii (TRIlong), and extensor carpi ulnaris (ECU)

- Inward direction: the subscapularis (SUBSC), teres major (TMAJ), sternocostal head of the pectoralis major (PECM2), abdominal head of the pectoralis major (PECM3), and pronator teres (PT)

Fig. 4.5 shows the muscles in the musculoskeletal model in OpenSim.

Fig. 4.6 shows an example of the muscle activity characteristics with respect to the applied force for each operating direction. The circles indicate the result at $0°$ of the lever angle, whereas the triangles indicate the result at the maximum lever angle in each operation direction. The dotted lines indicate approximate lines. These results suggest that the muscle activity is proportional to the applied force and that (10) is satisfied even during the lever operation. The slope k_j and intercept m_j of (10) were calculated using the least-squares method from the estimated value of the α for each F_a value at the lever angle j. R^2 was calculated using (19). Table 4.2 lists the coefficients k_j and m_j, and the coefficient of determination R^2.
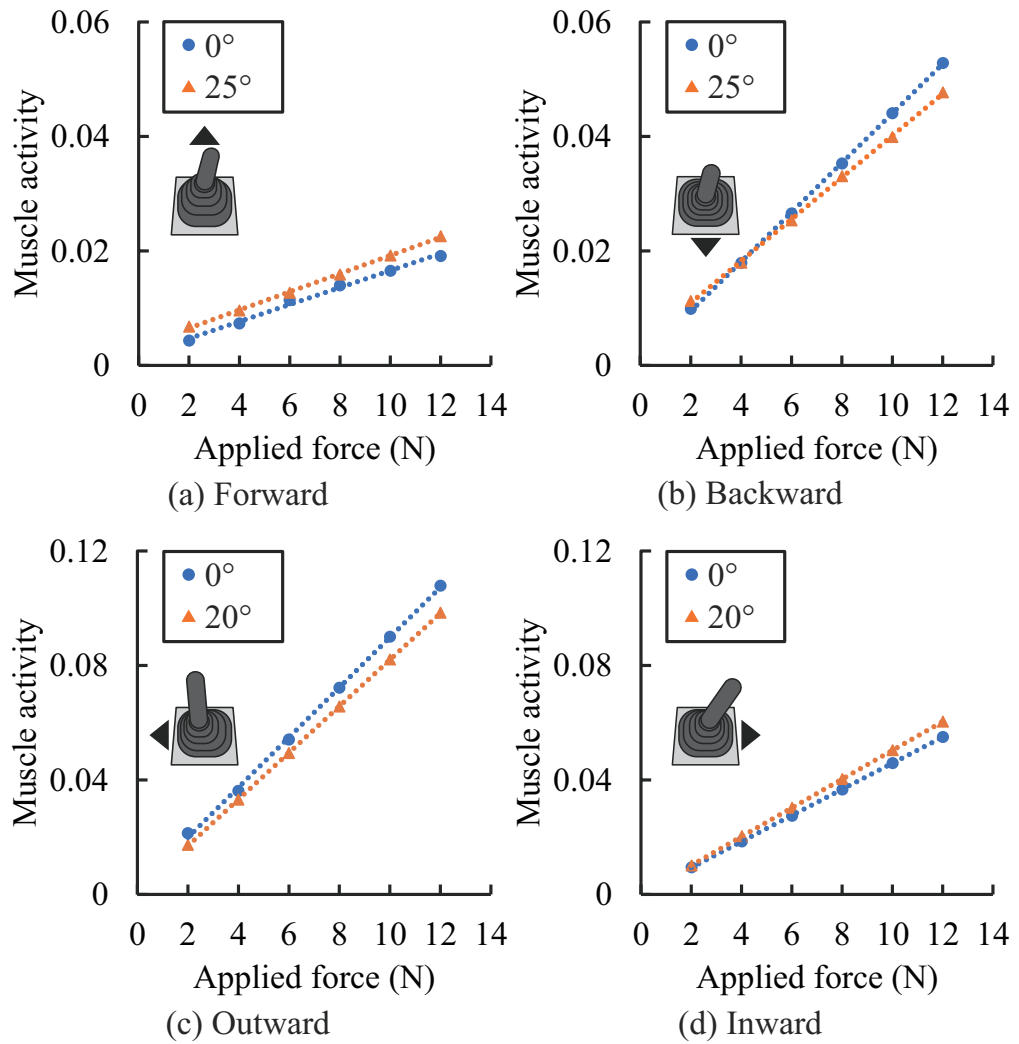
Fig. 4.6: Representative estimation results of activities of muscles that are actively involved when holding the lever. Circles and triangles indicate the results for 0° and the maximum lever angle in each operation direction, respectively.

4.2.5 Perceived Force Estimation during Lever Operation

The muscle activity was calculated when a force of 6 N was applied at each lever angle using (10) and the coefficients listed in Table 4.2. Also, the force perception-change ratio was determined by substituting the muscle activity at

Table 4.2: Coefficients k_j and m_j, and the coefficient of determination R^2.

	Forward			Backward		
j	k_j	m_j	R^2	k_j	m_j	R^2
0	0.00150	0.00159	0.992	0.00432	0.00088	1.000
2.5	0.00124	0.00317	1.000	0.00428	0.00096	1.000
5	0.00125	0.00343	1.000	0.00423	0.00132	1.000
7.5	0.00127	0.00315	1.000	0.00402	0.00298	0.999
10	0.00156	0.00218	0.988	0.00402	0.00262	0.999
12.5	0.00145	0.00246	0.981	0.00401	0.00262	0.999
15	0.00133	0.00350	1.000	0.00392	0.00302	0.999
17.5	0.00140	0.00330	0.999	0.00387	0.00320	1.000
20	0.00145	0.00344	0.999	0.00381	0.00338	1.000
22.5	0.00152	0.00347	0.999	0.00376	0.00348	0.999
25	0.00159	0.00337	0.999	0.00365	0.00366	1.000
	Outward			Inward		
j	k_j	m_j	R^2	k_j	m_j	R^2
0	0.00874	0.00246	0.999	0.00455	0.00033	1.000
2.5	0.00876	0.00088	1.000	0.00463	0.00012	1.000
5	0.00860	0.00085	1.000	0.00464	0.00050	1.000
7.5	0.00854	0.00085	1.000	0.00474	0.00018	1.000
10	0.00846	0.00083	1.000	0.00477	0.00020	1.000
12.5	0.00837	0.00082	1.000	0.00486	0.00023	1.000
15	0.00832	0.00082	1.000	0.00492	0.00022	1.000
17.5	0.00832	0.00084	1.000	0.00496	0.00021	1.000
20	0.00812	0.00084	1.000	0.00502	0.00021	1.000

each lever angle into (12) ($j = 0$). Fig. 4.7 shows the muscle activity and the force perception-change ratio with respect to the lever angle. Evidently, the muscle activity and force perception-change ratio change slightly according to the posture even when the same force is applied. The perceived force can be calculated using the force perception-change ratio and (13). Fig. 4.8 shows the relationship between the calculated perceived force, lever angle, and applied force. Evidently, the perceived force increases logarithmically as the applied force increases. Furthermore, the posture-changing effect according to the lever angle on the perceived force is comparatively small. We calculated the
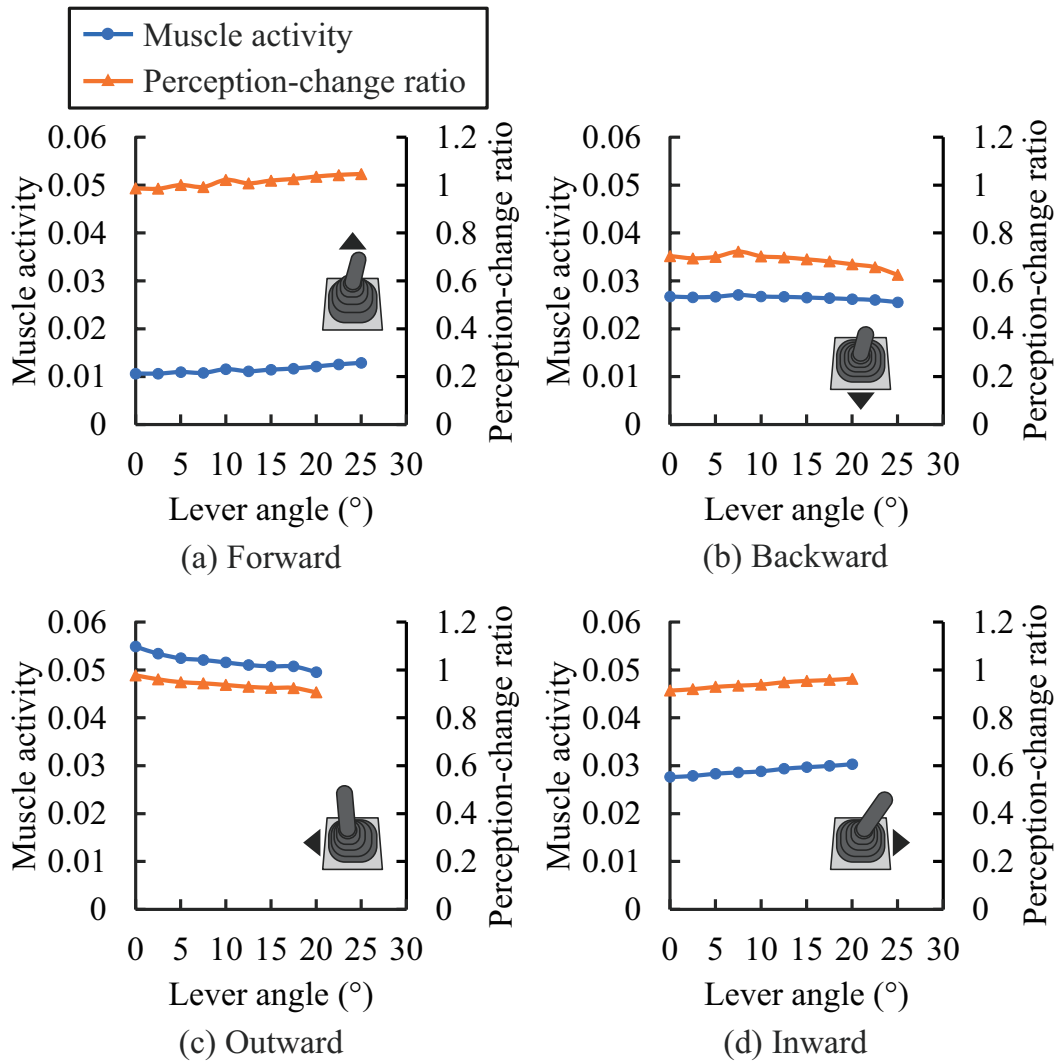
Fig. 4.7: Muscle activity and force perception-change ratio with respect to lever angle (6-N force is applied).

estimated perceived force for each angle of the conventional lever using this model and compared it with the measured perceived force.

The perceived force was measured using the magnitude estimation method [48]. The experimental environment was the same as described in Section 4.2.3 and shown in Fig. 4.2. However, the excavator lever was used instead of the force presentation lever. The experimental procedure is as follows:
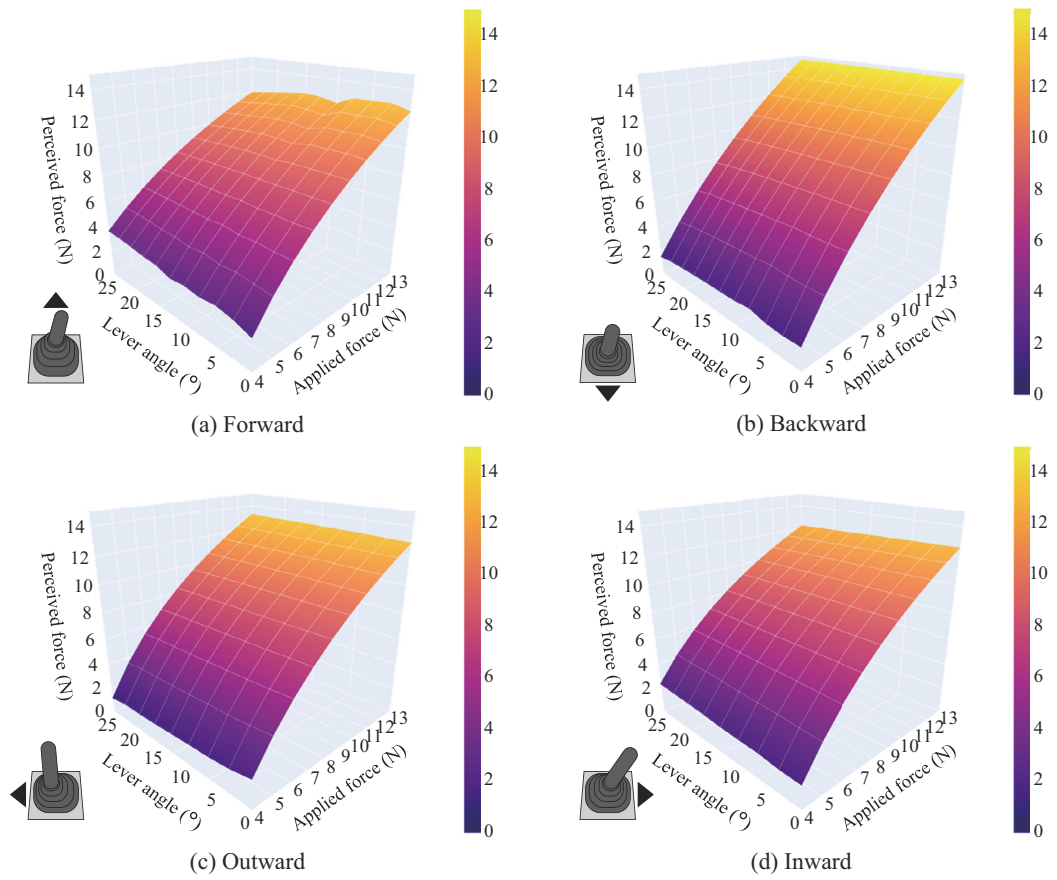
Fig. 4.8: Predicted perceived force with respect to lever angle and applied force.

1. The subjects sit on the seat and hold the lever with their left hand. Then, the subjects operate the lever to the target angle while looking at the displayed gauge, which shows the present and target angles of the lever, and holds the lever stationarily at the target angle for 5 s. Also, the subjects memorize the magnitude of the perceived force at that time. The first target angle is set to a standard angle. The display position of the target angle on the gauge is always set to the center to prevent the subject from judging the target angle using the gauge as much as possible.

2. The target angle is changed to the comparison angle, and the subject operates the lever as in step 1. Afterward, the subject reports the magnification of the perceived force for the comparison angle relative to the perceived force for the standard angle.

3. The standard angle is 12° forward and backward and 10° outward and inward. The comparison angles range from 6° to 20° forward and backward and from 4° to 16° outward and inward with an interval of 2°. The comparison angles are randomly displayed, and steps 1 and 2 are repeated until each comparison angle is displayed five times.

The above tasks were performed forward, backward, outward, and inward. The subjects were the same three subjects who participated in the experiment described in Section 4.2.3, and informed consent was obtained. The subjects practiced the experimental task for about 5 min before the experiment.

Fig. 4.9 shows the estimated and measured values of the perceived force for each lever angle. The circles indicate the estimated perceived force, the triangles indicate the measured perceived force, and the crosses indicate the reaction force of the lever. The root mean square percentage error (RMSPE) between the estimated and measured perceived force was determined to confirm the estimation accuracy. The cubic spline interpolation was used for the estimated values because the ranges and intervals of the estimated and measured values differed due to the experimental environment variation. The following are the RMSPE values: 5.7% for 6°–20° forward, 6.0% for 6°–20° backward, 7.8% for 4°–16° outward, and 14.3% for 4°–16° inward.
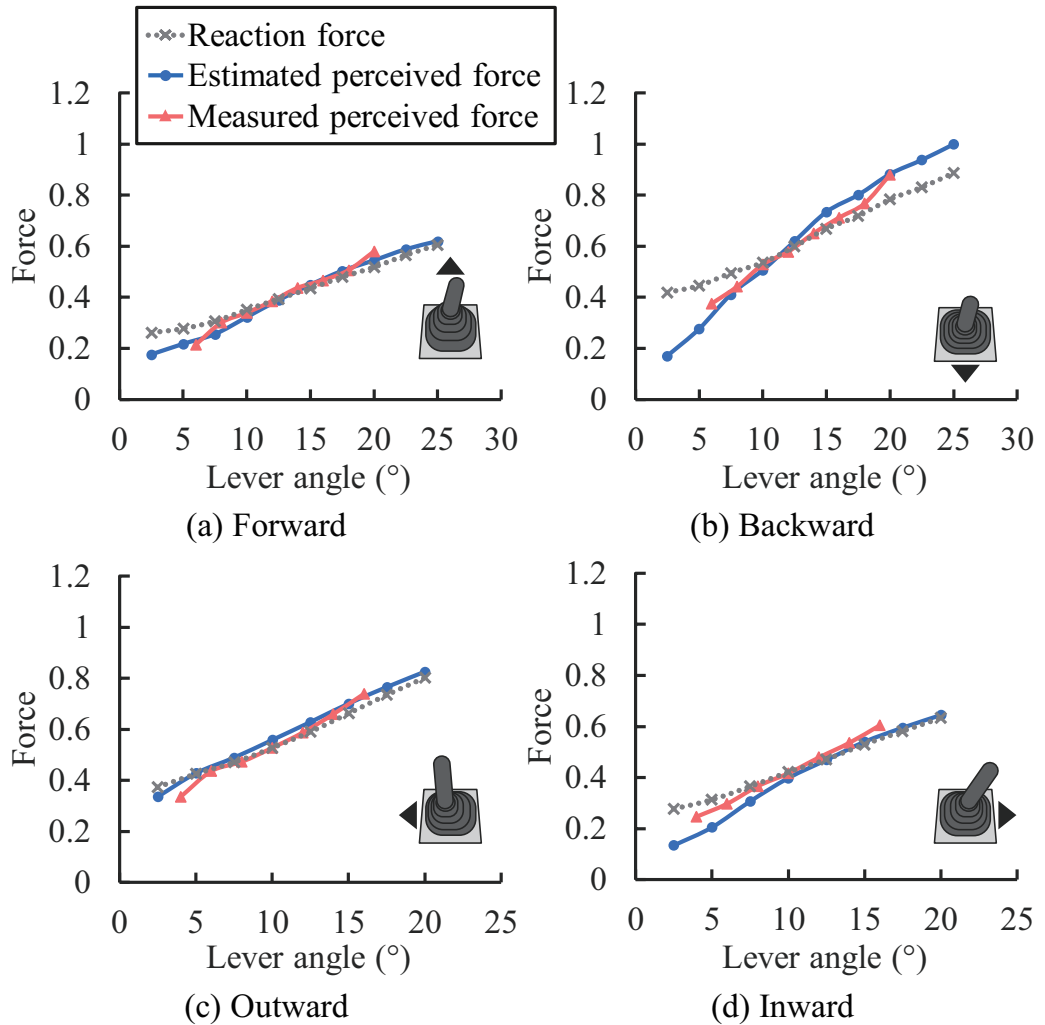
Fig. 4.9: Estimated and measured perceived forces of conventional lever. Each value was normalized by the maximum value of the estimated perceived force in four directions.

4.3 Verification of Lever Reaction Force Design Considering Force Perception Characteristics

4.3.1 Design of Lever Reaction Force

The reaction force of the lever was designed considering the force perception characteristics using the constructed prediction model of the perceived force.
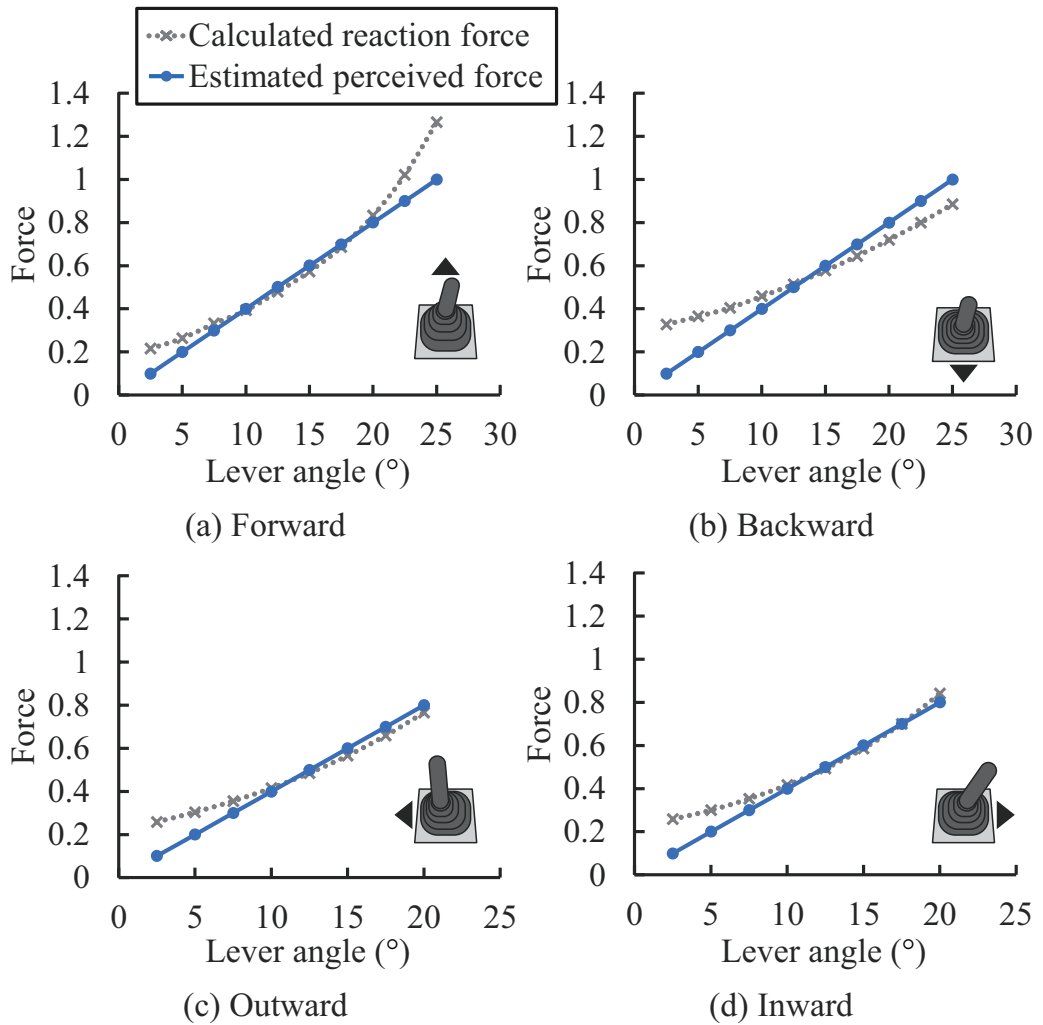
Fig. 4.10: Proposed perceived and calculated reaction force characteristics. Each value was normalized by the maximum value of the perceived force in four directions.

Fig. 4.9 shows that the conventional force perception characteristics are non-linear and asymmetric in all four directions: forward, backward, outward, and inward. These unreasonable and complicated characteristics may cause discomfort during the lever operation and make the excavator operation more difficult. Thus, we propose linear and symmetric reaction force characteristics in the forward, backward, outward, and inward directions. The reaction force

characteristics were calculated numerically from the target perceived force using the constructed model, as described in Section 4.2. Furthermore, the maximum value of the target perceived force equivalent was set to that of the conventional lever. Fig. 4.10 shows the proposed target perceived force and the calculated reaction force necessary to realize it. The circles and crosses indicate the proposed perceived and reaction forces, respectively.

4.3.2 Operating simulator of hydraulic excavator used for operability evaluation

The operability of the proposed reaction force design was evaluated using the operating simulator of a hydraulic excavator (Fig. 4.11). This simulator is similar to the simulator used in the previous study [19] except for the lever, seat, and display. The simulator was built using the game engine Unity, and the excavator could be operated with the force presentation levers (Fig. 4.1). The system of each operated joint of the hydraulic excavator was approximated as the first-order lag system with the dead time in the simulator. The 3D model of the excavator was created based on the CAD data of the 13-ton hydraulic excavator manufactured by Kobelco Construction Machinery Co., Ltd. The cab view of the excavator in the simulator was displayed on the screen. It has been reported that the results were similar to those of the real excavator when evaluating the digging work [19].

We investigated the presence of the cab view displayed on the screen and system usability when using the simulator instead of a real excavator. The reaction force characteristics of the force presentation lever were those of the conventional lever of a hydraulic excavator. Four male subjects (average age: 23.5 ± 1.7 years) who had experience operating a real excavator participated in the experiment. Informed consent was obtained from the subjects, and their

(a) Displayed screen   (b) Experiment environment

Fig. 4.11: Evaluation of the proposed perceived force characteristics using the simulator. The image shows the subject performing the leveling task. Informed consent was obtained from the individual for the publication of this image.

health conditions were verbally enquired. The subjects performed the leveling tasks by the simulator and answered the questionnaire. The leveling task entails moving the bucket tip parallel to the ground (Fig. 4.12). Herein, the bucket angle was fixed, and the leveling work was performed only by operating the boom and arm. The leveling task, which involved pulling and pushing, was repeated 10 times. The presence of the cab view displayed on the screen was evaluated using four items ("presence," "powerfulness," "comfortableness," and "depth") by referring to an evaluation questionnaire for the presence of a wide-field still image [50]. Each item was answered with a 7-point scale from 1 to 7, corresponding to "Bad," "Poor," "Fairly poor," "Fair," "Fairly good," "Good," and "Excellent." The system usability was evaluated using the System Usability Scale (SUS) [51]; a 10-item questionnaire for measuring a system's usability with a score ranging from 0 to 100.
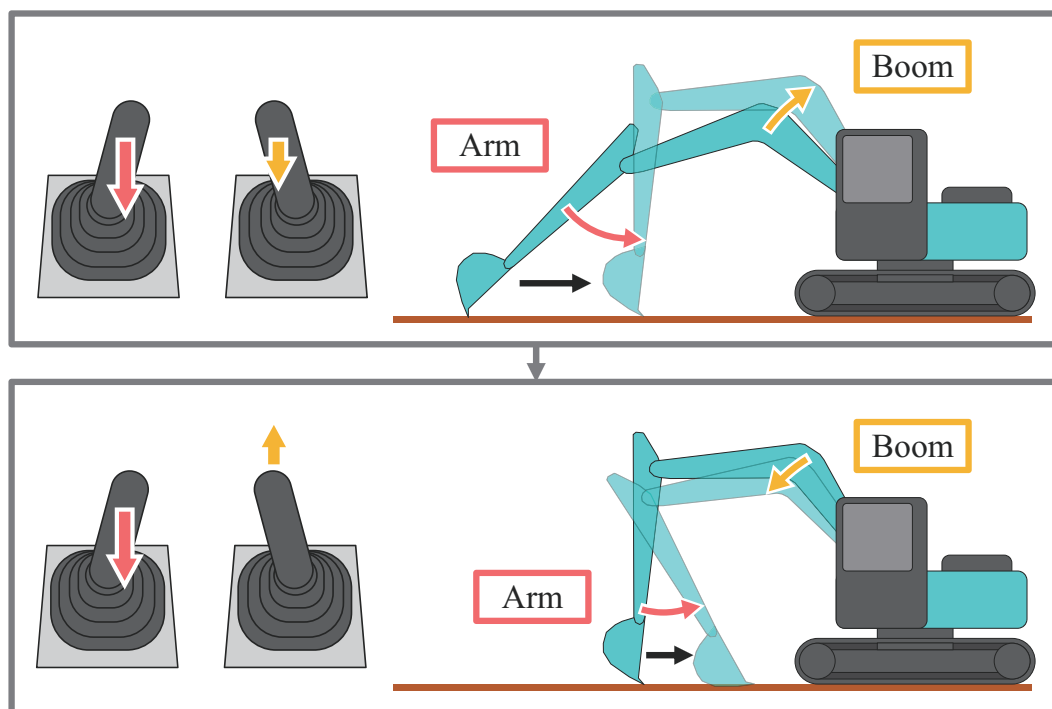
Fig. 4.12: Lever operation during the leveling task.

Table 4.3: Mean scores (standard deviation in parenthesis) for the presence of the cab view and system usability.

Item	Mean score (standard deviation)
Presence	5.00 (1.22)
Powerfulness	4.25 (0.83)
Comfatableness	5.50 (0.87)
Depth	3.75 (0.83)
SUS	80.00 (4.68)

Table 4.3 shows the mean scores for the presence of the cab view and system usability. Each number in parentheses represents the standard deviation. The mean scores of "presence" and "comfortableness" exceeded five points, corresponding to "Fairly good." The mean score of "powerfulness" exceeded four points, corresponding to "Fair," and that of "depth" was below four points. By performing the Student's one-sample t-test for the SUS score, a significant

difference from the test value of 68 (the standard average of SUS score) was confirmed. Although there was no room for improvement in the presence of the cab view, the system usability was high enough that the simulator could be used to evaluate the lever's operability instead of the real excavator.

4.3.3 Experimental Protocol

The operability of the excavator was evaluated using the simulator to verify the effectiveness of the proposed reaction force design. The leveling task, involving pulling and pushing, was repeated 10 times in the experiment. Fig. 4.11 shows a subject performing the leveling task. Seven male subjects (average age: 23.1 $\pm$ 1.4 years) who had no excavator experience participated in the experiment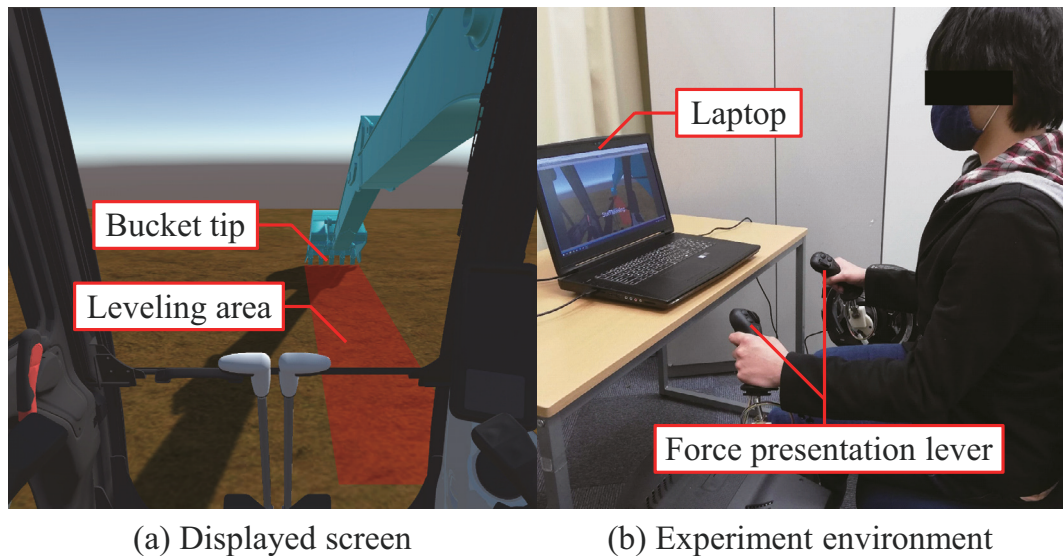. Informed consent was obtained from the subjects, and their health conditions were verbally enquired. Before the experiment, the subjects underwent one training session, in which the operating speed was controlled by reproducing the leveling operation performed by the expert on the simulator with the gauge of the lever operation amount assigned to the subjects. The leveling task was practiced 10 times by each of the inexperienced subjects. Three reaction forces were randomly applied for each subject: the proposed, conventional, and zero reaction forces. The conventional reaction force characteristics are the reaction force characteristics of the conventional hydraulic excavator's lever (Fig. 4.9). Herein, the operability of an excavator is considered from the following viewpoints: 1) how accurately the operators can operate, 2) how not tired they are during the operation, and 3) how much they can operate as they wish. The evaluation indices for operability are as follows.

- Mean bucket trajectory and dispersion of bucket trajectories: These indices were calculated using dynamic time warping (DTW) [39], a method

for calculating the dissimilarity between two time-series data, and DTW barycenter averaging [38], a method for calculating the average time-series data.

- Time: The time required for one leveling task was considered. This index was used to confirm whether the operation time was controlled.

- Mean absolute error (MAE): The mean absolute distance between the bucket tip and ground during one leveling task was calculated using the following equation.

$$MAE = \frac{1}{N} \sum_{i=0}^{N} |y_i|, \tag{20}$$

where $|y_i|$ is the absolute distance between the bucket tip and the ground, and N is the number of samples of data measured in one leveling task.

- Workload: The workload is the average score of six items in the Japanese version [34] of NASA-TLX [52]. The items were measured on a 101-point scale from 0 to 100.

- Sense of agency (SoA): The average score of 11 out of 21 items in the SoA scale for heavy machine operation [53], excluding items unrelated to the leveling task of the experiment, was considered. The items were measured on a 7-point scale from 1 to 7.

The questions for examining the workload and SoA are listed in Tables 4.4 and 4.5, respectively.

Table 4.4: Questions for examining the workload.

No.	Item
1	How much mental and perceptual activity was required?
2	How much physical activity was required?
3	How much time pressure did you feel due to the pace at which the tasks or task elements occurred?
4	How successful were you in performing the task?
5	How hard did you have to work to accomplish your level of performance?
6	How irritated, stressed, and annoyed versus content, relaxed, and complacent did you feel during the task?

Table 4.5: Questions for examining the sense of agency.

No.	Item
1	I operate the machine instinctively without thinking.
2	I operate the machine as if moving my arms and legs.
3	I can control and grasp the position of the machine's attachment or blade.
4	I feel the machine moves in correspondence to my lever operation.
5	I can operate according to the work process or goal I anticipated.
6	I can operate based on the machine's characteristic (inertia of the machine's movement, the machine's width, etc.)
7	I feel my operation is good.
8	I feel as if I could cause movement of the machine.
9	I feel as if I could control the movements of the machine.
10	The machine is obeying my will and I can make it move just like I want it.
11	I operate the machine carefully.

4.3.4 Result

Fig. 4.13 shows the mean bucket trajectory and dispersion of the trajectory during the leveling task (pulling direction) for subjects A, B, F, and G as an example. The solid gray lines indicate the mean trajectory with no reaction

(a) Sub. A

(b) Sub. B

(c) Sub. F

(d) Sub. G
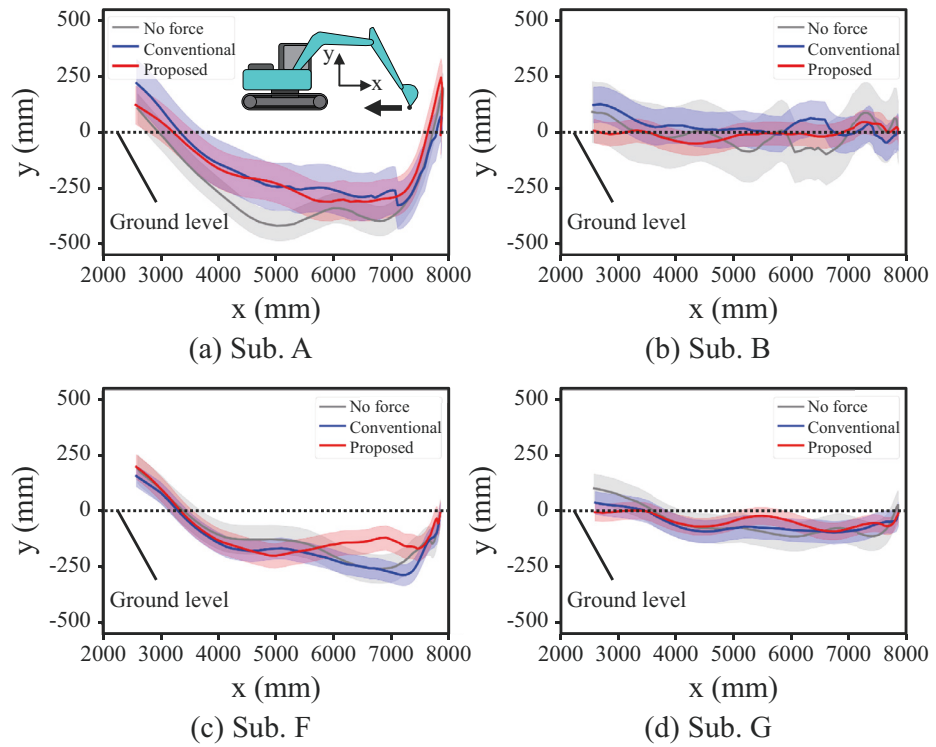
Fig. 4.13:　Mean bucket trajectory in leveling task for each subject (pulling direction).
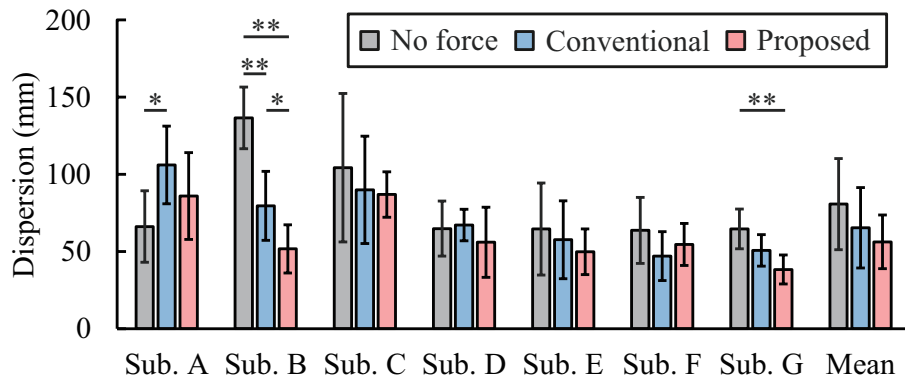
Fig. 4.14:　Dispersion of bucket trajectories in leveling task for each subject (pulling direction, *: $p < 0.05$, **: $p < 0.01$).

force, and the solid blue lines indicate the mean trajectory as per the conventional reaction force. Furthermore, the solid red lines indicate the mean trajectory as per the proposed reaction force. The semitransparent areas indicate the bucket trajectory dispersion. Also, the black dotted lines indicate the ground level. The results show that the trajectories achieved by applying the proposed reaction force are smooth curves and tend to be the closest to the ground. Fig. 4.14 shows the dispersion of the bucket trajectories in the pulling direction of the leveling task for each subject and the mean dispersion for all subjects. The asterisks on the graph indicate significant differences (*: $p < 0.05$, **: $p < 0.01$, one-way analysis of variance [ANOVA] followed by the Student's t-test with adjusted p values by the Holm method [54]). The dispersion for the proposed reaction force was the smallest though there was no significant difference between the three conditions in the mean dispersion of the trajectories of all subjects.

Fig. 4.15 shows the averages of the time, MAE, workload, and SoA for all the subjects. The error bar represents the standard deviation of the values for all subjects. The p values on the graph indicate significant differences at the 5% level (one-way ANOVA followed by the Student's t-test with adjusted p values by the Holm method [54]). There was no significant difference in the time between the three conditions because the operating speed was controlled in the experiment. It was confirmed that the MAE for the proposed reaction force was significantly less than that for the other. There was no significant difference in the workload between the three conditions, but the workload for the proposed reaction force was the least. Furthermore, the SoA for the proposed reaction force was significantly lower than that for the other. These results suggest that the linear and symmetric reaction force design improves the working accuracy and SoA.
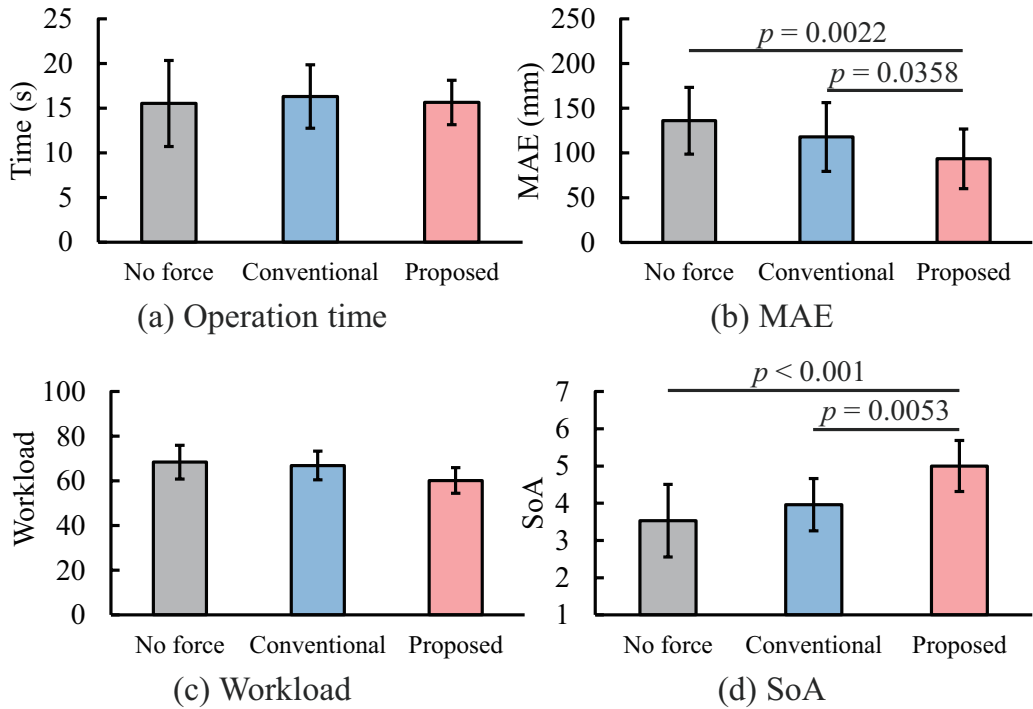
Fig. 4.15: Evaluation results for each reaction force characteristics in the leveling task.

4.4 Discussion

In this study, we conducted an experiment in which subjects answered their perceived force during the lever operation. We also constructed a model to predict the perceived force from the muscle activity estimated based on the posture and reaction force during the lever operation. This method has been proposed to estimate the perceived steering wheel operation force [32]. It has also been shown to be capable of explaining the force perception bias during the steering wheel operation [33]. We considered that this method could be applied to estimate the perceived force during the lever operation and designed the experiment for this study.

The perceived force differs depending on the operating direction, even for

identical magnitudes of the lever reaction force (Fig. 4.3). Meanwhile, Fig. 4.8 shows that the perceived force is less affected by the lever angle in all operating directions. Fig. 4.6 indicates that muscle activity has the same tendency as the perceived force. These results are supported by the fact that the magnitude of effort is strongly correlated with the judgment of force, as reported by McCloskey *et al.* [29], and by the neurophysiological evidence that muscle activity and sense of effort are correlated, as reported by Morree *et al.* [31]. Fig. 4.9 shows the estimated and measured values of the perceived force for each lever angle. The perceived force can be estimated with RMSPE values of 5.7% and 6.0% in the range of 6°–20° forward and backward, respectively, and 7.8% and 14.3% in the range of 4°–16° outward and inward, respectively. This result indicates that the subjectively perceived force during the lever operation can be predicted computationally. When using conventional techniques, it is necessary to conduct an experiment in which the subjects report the perceived forces for all lever angles to conventionally obtain the force perception characteristics during the lever operation. Furthermore, the perceived force can be computationally estimated from musculoskeletal simulation without subject experimentation using the proposed method. The proposed method allows us to obtain the force perception quantity at a lower experimental cost than the conventional method. Fig. 4.10 shows the proposed perceived and calculated reaction forces. As mentioned above, the perceived force characteristics differ depending on the operating direction. The reaction force characteristics vary directionally when the force perception characteristics are identical in all directions. Furthermore, the relationship between the reaction and perceived forces can be roughly explained by the Weber–Fechner law [40], regardless of the lever angle because the effect of the lever angle on force the perception is small. Therefore, the calculated reaction force is approximately proportional

to the exponential function of the lever angle. In this study, we hypothesized that the reaction force design in which the perceived force varies linearly with the lever angle improved the operability of the leveling operation of the excavator. Indeed, our results verify this hypothesis. Fig. 4.13 shows an example of the bucket trajectory. As per the proposed force perception characteristics, the trajectory is the closest to the ground and is a smooth curve. The results in Fig. 4.15 indicate that the linear and symmetric reaction force design improves the working accuracy and SoA in the leveling operation. These results may be attributed to the proper design of the force perception characteristics of the lever. Consequently, this finding supports the study's hypothesis.

However, the perceived force estimation method used for the reaction force design in this study has some limitations. First, the proposed method does not consider individual differences, such as the operator's physique and operational proficiency. The perceived force was estimated in the fixed posture using a standard human musculoskeletal model. However, the parameters, such as bone length and origin of each muscle, differ per person, and the operating posture also changes depending on the physique. Since the method adopted in this study depends on the simulation accuracy of the muscle activity, if the human body model is hugely different from the operator's physique, the estimation accuracy of the perceived force may decrease. Moreover, we did not verify the effectiveness of the proposed reaction force characteristics for operators who are accustomed to the lever of the conventional reaction force characteristics. The skilled and nonskilled operators may operate the same lever in different postures and with varying usages of muscles. Muscle co-contraction controls the joint stiffness [55] and helps humans realize accurate movements [56, 57]. Osu *et al.* showed that co-contraction gradually decreases during the learning process of a new motor task [58]. This finding suggests that the skilled

operator operates the lever with less muscle force. Since co-contraction is not considered in the musculoskeletal simulation used in the proposed method, the estimation accuracy of muscle activity may decrease, especially for operators who are unaccustomed to operating excavators. Using a musculoskeletal model suitable for the operator's physique and considering muscle co-contraction is essential for improving the estimation accuracy of muscle activity. Also, it is necessary to verify the effectiveness of the proposed perceived force characteristics for an operator who is sufficiently accustomed to the lever of the conventional perceived force characteristics. Second, only static musculoskeletal simulations were performed in this study. However, in reality, the lever operation involves dynamic postural changes. Mitchell *et al.* reported that dynamic exercises involve changes in muscle length and joint movement with rhythmic contractions, resulting in reduced intramuscular forces compared to those involved in static exercises [59]. Muscle activity characteristics differ depending on whether the movement is dynamic or static. Dynamic musculoskeletal simulations require sophisticated algorithms. Third, although the results of efferent signals, i.e., muscle activity, were used to estimate the force perception in this study, afferent signals from muscle spindles and peripheral skin receptors are also essential factors in determining a sense of force [60–62]. As described in Section 4.1, muscle activity as a sense of effort can be used to predict the sense of force. However, Phillips *et al.* proposed that the sense of force should be predicted based on the sense of effort and the afferent feedback from the periphery [63]. Monjo *et al.* proposed that humans do not perceive only efferent or afferent signals as a sense of effort; in fact, the sense of effort is perceived by changes in the balance of the two signals according to the experimental conditions [64]. The sense of force may be altered by the influence of afferent signals from peripheral skin receptors due to skin vibration and

deformation in the case of a lever in the cab to which the engine vibration transmits, or a lever implemented with vibration feedback [65, 66] or skin deformation feedback [67–69]. Hence, it is essential to consider afferent signals from muscle spindles and peripheral skin receptors to improve the estimation accuracy of force perception. Fourth, the force perception in the combined operation of the longitudinal and lateral directions remains unverified. It may be difficult to perceive the reaction force in the longitudinal and lateral directions independently due to the duplication between the active muscles when operating the lever in these directions. Building a lever corresponding to two axes is necessary because the force presentation lever used in this study has only one axis. A lever reaction force design more suitable for determining the human force perception characteristics can be realized by solving these problems.

Moreover, in this study, only the simulator was used to verify the operability of the proposed reaction force lever, and it is uncertain whether the same results can be obtained in the real excavator. The verification using a real excavator will be included in future work.

4.5 Conclusion

In this study, we proposed a lever reaction force design considering human force perception characteristics. We estimated the force perception characteristics in operating a lever of an excavator by muscle activity estimation using musculoskeletal simulation. The results showed that the perceived force in the lever operation could be computationally predicted. We evaluated the lever reaction force characteristics designed based on the clarified force perception characteristics. Furthermore, we confirmed that the reaction force design in which the force perception characteristics are linear and symmetric in each

direction improved the operability of the excavator's leveling operation. In the future, we will estimate the perceived force considering the combined operation of the longitudinal and lateral directions of the lever and evaluate the operability in other tasks, such as excavation work. Furthermore, we will verify the operability of the proposed reaction force lever with a real excavator.

Chapter 5

Conclusions

In this paper, we worked on the development of the operation training system and the improvement of the operability of hydraulic excavators in order to improve the operators' skills of hydraulic excavators. The followings are summaries and conclusions for each chapter of the dissertation.

In Chapter 2, we developed the operation training system using an RC toy excavator and VR technology with the same viewpoint and operating interface as a real excavator. We investigated the dynamic characteristics of the RC toy excavator used in the developed system. The results showed that the dynamic characteristics of the RC toy excavator are significantly different from those of the real excavator. Next, we evaluated the operability and presence of the developed system by questionnaire. The results indicate that the experienced operators find it more difficult to operate the RC toy excavator and tend to give lower scores for presence and comfort. The reason for these results may be that the experienced operators felt a sense of incongruity in the RC toy excavator that differs in operability and visibility from real excavators.

In Chapter 3, we verified indices that can quantitatively evaluate the operation skill of a real excavator using the RC toy excavator. We calculated evaluation indices for lever operation and bucket movement during excavation

using the proposed system and a real excavator. Although the dynamics were largely different, the results showed a high correlation between the RC toy excavator and real excavator in some operations and suggested that the proposed system could evaluate the operational skills with regard to the correspondence between the direction of the lever and the joint angle of the excavator.

In Chapter 4, we proposed a lever reaction force design considering human force perception characteristics. We estimated the force perception characteristics in operating a lever of an excavator by muscle activity estimation using musculoskeletal simulation. The results showed that the perceived force in the lever operation could be computationally predicted. We evaluated the lever reaction force characteristics designed on the basis of the clarified force perception characteristics. In addition, we confirmed that the reaction force design in which the force perception characteristics are linear and symmetric in each direction improved the operability of the leveling operation of the excavator.

However, the operation training system and the lever reaction force design method proposed in this paper have some limitations. There are following two limitations to the proposed training system. First, the proposed system does not completely reproduce the operability of the real excavator. The dynamic characteristics of the RC toy excavator are significantly different from those of the real excavator. Moreover, the operation interface was reproduced with the gaming joysticks that have different stiffness from the real lever.

Second, the proposed system does not completely reproduce the field of view from the operator's seat. We replaced the original human vision by the HMD and omnidirectional camera with much lower resolution than the human eye. The current system was not capable of providing depth information. Nevertheless, the evaluation of depth perception was not much worse because

the depth was perceived in a monocular image with the help of environmental conditions such as lighting, shadows, etc. In addition, the latency of the visual system has a great influence on visual immersion. In order to enable more effective training and accurate skill evaluation, it is necessary to closely reproduce the operability and visibility of real excavators in the RC toy excavator.

Third, this study is limited to the evaluation of the operation skills of hydraulic excavators using the RC toy excavator, and it has not been verified whether effective training can actually be performed using it. It is necessary to verify the training effect of the RC toy excavator by observing the changes in the operation skills over time with such training.

There are following four limitations in the proposed lever reaction force design method. First, the proposed method does not consider individual differences, such as the operator's physique and operational proficiency. The perceived force was estimated in the fixed posture using a standard human musculoskeletal model. However, the parameters, such as bone length and origin of each muscle, differ per person, and the operating posture also changes depending on the physique. Since the method adopted in this study depends on the simulation accuracy of the muscle activity, if the human body model is hugely different from the operator's physique, the estimation accuracy of the perceived force may decrease. Moreover, we did not verify the effectiveness of the proposed reaction force characteristics for operators who are accustomed to the lever of the conventional reaction force characteristics. The skilled and nonskilled operators may operate the same lever in different postures and with varying usages of muscles. Muscle co-contraction controls the joint stiffness [55] and helps humans realize accurate movements [56,57]. Osu *et al.* showed that co-contraction gradually decreases during the learning process of a new motor task [58]. This finding suggests that the skilled operator operates the lever

with less muscle force. Since co-contraction is not considered in the muscu-loskeletal simulation used in the proposed method, the estimation accuracy of muscle activity may decrease, especially for operators who are unaccustomed to operating excavators. Using a musculoskeletal model suitable for the opera-tor's physique and considering muscle co-contraction is essential for improving the estimation accuracy of muscle activity. Also, it is necessary to verify the effectiveness of the proposed perceived force characteristics for an operator who is sufficiently accustomed to the lever of the conventional perceived force characteristics.

Second, only static musculoskeletal simulations were performed in this study. However, in reality, the lever operation involves dynamic postural changes. Mitchell *et al.* reported that dynamic exercises involve changes in muscle length and joint movement with rhythmic contractions, resulting in re-duced intramuscular forces compared to those involved in static exercises [59]. Muscle activity characteristics differ depending on whether the movement is dynamic or static. Dynamic musculoskeletal simulations require sophisticated algorithms.

Third, although the results of efferent signals, i.e., muscle activity, were used to estimate the force perception in this study, afferent signals from muscle spindles and peripheral skin receptors are also essential factors in determining a sense of force [60–62]. As described in Section 4.1, muscle activity as a sense of effort can be used to predict the sense of force. However, Phillips *et al.* proposed that the sense of force should be predicted based on the sense of effort and the afferent feedback from the periphery [63]. Monjo *et al.* proposed that humans do not perceive only efferent or afferent signals as a sense of effort; in fact, the sense of effort is perceived by changes in the balance of the two signals according to the experimental conditions [64]. The sense of force may

be altered by the influence of afferent signals from peripheral skin receptors due to skin vibration and deformation in the case of a lever in the cab to which the engine vibration transmits, or a lever implemented with vibration feedback [65, 66] or skin deformation feedback [67–69]. Hence, it is essential to consider afferent signals from muscle spindles and peripheral skin receptors to improve the estimation accuracy of force perception.

Fourth, the force perception in the combined operation of the longitudinal and lateral directions remains unverified. It may be difficult to perceive the reaction force in the longitudinal and lateral directions independently due to the duplication between the active muscles when operating the lever in these directions. Building a lever corresponding to two axes is necessary because the force presentation lever used in this study has only one axis. A lever reaction force design more suitable for determining the human force perception characteristics can be realized by solving these problems.

Finally, the future prospects are described. In recent years, telework will be promoted from the perspective of workstyle reforms and infectious disease control. And also, with the development of IT systems, digital matching services that are different from conventional industries such as Uber have appeared, and the variety of working styles is expanding. In the construction industry, it is essential to secure and retain new employees due to the effects of the declining birthrate and aging population. It is expected that the system that enables telework will transform the construction industry into a site where anyone can work anywhere. Therefore, the teleoperation of construction equipment is noticed in the construction industry. Ito *et al.* have developed a cross-platform cockpit system for teleoperated excavators [12]. We would like to construct an environment that can easily carry out the operation training of the teleoperated excavator by enabling the operation of the RC toy excavator using this

cockpit system. And also, since there is less information to be fed back in the teleoperation of the excavator in comparison with the boarding operation, the technology which supplements these is necessary. We would like to propose a more intuitive force feedback method using the lever reaction force design method considering force perception characteristics proposed in this study.

Chapter 6

Appendix

6.1 DTW

The DTW is a method of calculating the distance between two time series of different lengths. An example of using the DTW algorithm to calculate the distance of two time series data ($A = \{a_1, a_2, \cdots, a_I\}$, and $B = \{b_1, b_2, \cdots, b_J\}$) is presented below.

Step 1   The distance $d(a_1, b_1)$ between a_1 and b_1 is calculated; this is the DTW distance $D(1, 1)$.

Step 2   The DTW distance $D(i, 1)$ is calculated in order as follows:

$$D(i, 1) = D(i - 1, 1) + d(a_i, b_1). \tag{21}$$

$$i = 2, 3, \cdots, I. \tag{22}$$

Step 3   The DTW distance $D(1, j)$ is calculated in order as follows:

$$D(1, j) = D(1, j - 1) + d(a_1, b_j). \tag{23}$$

$$j = 2, 3, \cdots, J. \tag{24}$$

Step 4 The DTW distance $D(i, j)$ is calculated in order as follows:

$$D(i, j) = min \left\{ \begin{array}{c} D(i, j-1) \\ D(i-1, j) \\ D(i-1, j-1) \end{array} \right\} + d(a_i, b_j). \tag{25}$$

$$i = 2, 3, \cdots, I, \quad j = 2, 3, \cdots, J. \tag{26}$$

Then, $D(I, J)$ is the DTW distance of time series A and B. The smaller this value, the more similar will the two time series data be. The correspondence between the points of time series A and B was obtained by calculating $D(I, J)$ and is called the warping path.

In this study, the distance function $d(a_i, b_j)$ could be varied according to the type of time series data. The distance in 3D Euclidean space, which is expressed by the following equation, was used to handle the 3D trajectory data.

$$d(a_i, b_j) = $$
$$\sqrt{(a_{i1} - b_{j1})^2 + (a_{i2} - b_{j2})^2 + (a_{i3} - b_{j3})^2}. \tag{27}$$
$$a_i = (a_{i1}, a_{i2}, a_{i3}), \quad b_j = (b_{j1}, b_{j2}, b_{j3}). \tag{28}$$

The value obtained by dividing the calculated DTW distance by the number of elements of the warping path was considered as the dissimilarity between the two trajectories to eliminate the influence of the number of elements in the trajectory data.

6.2 DBA

The DBA is a method of calculating the average time series of multiple time series data. An example of using the algorithm to calculate the average of the three time series ($A = \{a_1, a_2, \cdots, a_I\}$, $B = \{b_1, b_2, \cdots, b_J\}$, and $C = \{c_1, c_2, \cdots, c_K\}$) is presented below.

Step 1 Let us consider the arbitrary time series data as the provisional average time series data $M = \{m_1, m_2, \cdots, m_H\}$.

Step 2 The warping path of the average time series data and each time series data are calculated using the DTW method.

Step 3 Each point in the average time series is updated to the average value of points in each time series correlated by the warping path.

For example, m_h is updated with the warping path using the following expression with respect to data points a_i, b_j, and c_k associated with data point m_h.

$$m_h = \frac{a_i + b_j + c_k}{3}. \tag{29}$$

Step 4 Steps 2 and 3 are repeated until the average time series converges.

Bibliography

[1] M. Kamezaki, H. Iwata, and S. Sugano, "Development of an operation skill-training simulator for double-front work machine," in *Advanced Intelligent Mechatronics, 2008. AIM 2008. IEEE/ASME International Conference on.* IEEE, 2008, pp. 170–175.

[2] X. Wang, P. S. Dunston, R. Proctor, L. Hou, and J. So, "Reflections on using a game engine to develop a virtual training system for construction excavator operators," in *Proceedings of the 28th International Symposium on Automation and Robotics in Construction (ISARC 2011): Seoul, Korea*, 2011.

[3] T. Ni, H. Zhang, C. Yu, D. Zhao, and S. Liu, "Design of highly realistic virtual environment for excavator simulator," *Computers & Electrical Engineering*, vol. 39, no. 7, pp. 2112–2123, 2013.

[4] P. Vähä and M. Skibniewski, "Dynamic model of excavator," *Journal of aerospace engineering*, vol. 6, no. 2, pp. 148–158, 1993.

[5] D. Vujic, O. Lazarevic, and V. Batinic, "Development of dynamic-mathematical model of hydraulic excavator," *Journal of Central South University*, vol. 24, no. 9, pp. 2010–2018, 2017.

[6] B. P. Patel and J. M. Prajapati, "Soil-tool interaction as a review for

digging operation of mini hydraulic excavator," *International Journal of Engineering Science and Technology*, vol. 3, no. 2, pp. 894–901, 2011.

[7] L. Bernold, J. Lloyd, and M. Vouk, "Equipment operator training in the age of internet2," *Nist special publication sp*, pp. 505–510, 2003.

[8] Y. Sakaida, D. Chugo, H. Yamamoto, and H. Asama, "The analysis of excavator operation by skillful operator-extraction of common skills," in *SICE Annual Conference, 2008.* IEEE, 2008, pp. 538–542.

[9] K. Koiwai, T. Yamamoto, T. Nanjo, Y. Yamazaki, and Y. Fujimoto, "Data-driven human skill evaluation for excavator operation," in *2016 IEEE International Conference on Advanced Intelligent Mechatronics (AIM).* IEEE, 2016, pp. 482–487.

[10] A. Hosseini and M. Lienkamp, "Enhancing telepresence during the tele-operation of road vehicles using hmd-based mixed reality," in *2016 IEEE Intelligent Vehicles Symposium (IV).* IEEE, 2016, pp. 1366–1373.

[11] A. Sawarkar, V. Chaudhari, R. Chavan, V. Zope, A. Budale, and F. Kazi, "Hmd vision-based teleoperating ugv and uav for hostile environment using deep learning," *arXiv preprint arXiv:1609.04147*, 2016.

[12] M. Ito, Y. Funahara, S. Saiki, Y. Yamazaki, and Y. Kurita, "Development of a cross-platform cockpit for simulated and tele-operated excavators," *Journal of Robotics and Mechatronics*, vol. 31, no. 2, pp. 231–239, 2019.

[13] J. Kunieda and Y. Hoshino, "Development of rc helicopter control skill study support system in consideration of user interface," in *2009 IEEE International Conference on Fuzzy Systems.* IEEE, 2009, pp. 957–962.

[14] R. Takaseki, N. Sano, R. Nagashima, and T. Okazaki, "Basic study on override ship maneuvering simulator using actual training ship," *Proceedings of the Japan Joint Automatic Control Conference*, vol. 57, pp. 1493–1497 (in Japanese), 2014.

[15] M. E. Altinsoy and S. Merchel, "Audiotactile feedback design for touch screens," in *International Conference on Haptic and Audio Interaction Design*. Springer, 2009, pp. 136–144.

[16] Y. Song, S. Guo, X. Yin, L. Zhang, H. Hirata, H. Ishihara, and T. Tamiya, "Performance evaluation of a robot-assisted catheter operating system with haptic feedback," *Biomedical Microdevices*, vol. 20, no. 2, pp. 1–16, 2018.

[17] M. Haruna, M. Ogino, and T. Koike-Akino, "Proposal and evaluation of visual haptics for manipulation of remote machine system," *Frontiers in Robotics and AI*, vol. 7, 2020.

[18] M. Ito, C. Raima, S. Saiki, Y. Yamazaki, and Y. Kurita, "A study on machine instability feedback during digging operation in teleoperated excavators," in *2020 13th International Conference on Human System Interaction (HSI)*. IEEE, 2020, pp. 14–19.

[19] ——, "Effects of machine instability feedback on safety during digging operation in teleoperated excavators," *IEEE Access*, vol. 9, pp. 28 987–28 998, 2021.

[20] Y.-J. Nam and M.-K. Park, "Virtual excavator simulator featuring hils and haptic joysticks," *Journal of Mechanical Science and Technology*, vol. 29, no. 1, pp. 397–407, 2015.

[21] D. Q. Truong, B. N. M. Truong, N. T. Trung, S. A. Nahian, and K. K. Ahn, "Force reflecting joystick control for applications to bilateral tele-operation in construction machinery," *International Journal of Precision Engineering and Manufacturing*, vol. 18, no. 3, pp. 301–315, 2017.

[22] M. CS, P. S. Sairam, V. Veeramalla, A. Kumar, and M. K. Gupta, "Design and analysis of new haptic joysticks for enhancing operational skills in excavator control," *Journal of Mechanical Design*, vol. 142, no. 12, p. 121406, 2020.

[23] Z. Chen, F. Huang, C. Yang, and B. Yao, "Adaptive fuzzy backstepping control for stable nonlinear bilateral teleoperation manipulators with enhanced transparency performance," *IEEE transactions on industrial electronics*, vol. 67, no. 1, pp. 746–756, 2019.

[24] J. Guo, L. He, and S. Guo, "Study on force feedback control of the vascular interventional surgical robot based on fuzzy pid," in *2020 IEEE International Conference on Mechatronics and Automation (ICMA)*. IEEE, 2020, pp. 1710–1715.

[25] A. Sayadi, A. Hooshiar, and J. Dargahi, "Impedance matching approach for robust force feedback rendering with application in robot-assisted interventions," in *2020 8th International Conference on Control, Mechatronics and Automation (ICCMA)*. IEEE, 2020, pp. 18–22.

[26] K. Takemura, N. Yamada, A. Kishi, K. Nishikawa, T. Nouzawa, Y. Kurita, and T. Tsuji, "Kansei-related assessment in a subjective force perception space and its application to a design for steering wheel operation characteristics (in japanese)," *Transactions of the Society of Automative Engineers of Japan*, vol. 81, no. 822, pp. 14–00463, 2015.

[27] L. A. Jones, "Perception of force and weight: theory and research." *Psychological bulletin*, vol. 100, no. 1, p. 29, 1986.

[28] K. Takemura, N. Yamada, A. Kishi, K. Nishikawa, T. Nouzawa, C. Li, Y. Kurita, and T. Tsuji, "A subjective force perception model of humans and its application to a steering operation system of a vehicle," in *2013 IEEE International Conference on Systems, Man, and Cybernetics*. IEEE, 2013, pp. 3675–3680.

[29] D. McCloskey, S. Gandevia, E. Potter, and J. Colebatch, "Muscle sense and effort: motor commands and judgments about muscular contractions." *Advances in Neurology*, vol. 39, pp. 151–167, 1983.

[30] E. Cafarelli and B. Bigland-Ritchie, "Sensation of static force in muscles of different length," *Experimental neurology*, vol. 65, no. 3, pp. 511–525, 1979.

[31] H. M. De Morree, C. Klein, and S. M. Marcora, "Perception of effort reflects central motor command during movement execution," *Psychophysiology*, vol. 49, no. 9, pp. 1242–1253, 2012.

[32] Y. Kishishita, K. Takemura, N. Yamada, T. Hara, A. Kishi, K. Nishikawa, T. Nouzawa, T. Tsuji, and Y. Kurita, "Prediction of perceived steering wheel operation force by muscle activity," *IEEE transactions on haptics*, vol. 11, no. 4, pp. 590–598, 2018.

[33] Y. Kishishita, Y. Tanaka, and Y. Kurita, "Force perceptual bias caused by muscle activity in unimanual steering," *PloS one*, vol. 14, no. 10, p. e0223930, 2019.

[34] S. Haga and N. Mizukami, "Japanese version of nasa task load index

sensitivity of its workload score to difficulty of three different laboratory tasks," *The Japanese journal of ergonomics*, vol. 32, no. 2, pp. 71–79, 1996.

[35] M. Emoto, K. Masaoka, M. Sugawara, and Y. Nojiri, "The viewing angle dependency in the presence of wide field still image viewing and its relationship to the evaluation indices," *The journal of the Institute of Image Information and Television Engineers*, vol. 60, no. 8, pp. 1288–1295 (in Japanese), 2006.

[36] W. Winn, "Learning in artificial environments: Embodiment, embeddedness and dynamic adaptation," *Technology, Instruction, Cognition and Learning*, vol. 1, no. 1, pp. 87–114, 2003.

[37] K. Kilteni, R. Groten, and M. Slater, "The sense of embodiment in virtual reality," *Presence: Teleoperators and Virtual Environments*, vol. 21, no. 4, pp. 373–387, 2012.

[38] F. Petitjean, A. Ketterlin, and P. Gançarski, "A global averaging method for dynamic time warping, with applications to clustering," *Pattern Recognition*, vol. 44, no. 3, pp. 678–693, 2011.

[39] H. Sakoe and S. Chiba, "Dynamic programming algorithm optimization for spoken word recognition," *IEEE transactions on acoustics, speech, and signal processing*, vol. 26, no. 1, pp. 43–49, 1978.

[40] G. T. Fechner, D. H. Howes, and E. G. Boring, *Elements of psychophysics*. Holt, Rinehart and Winston New York, 1966, vol. 1.

[41] S. L. Delp, F. C. Anderson, A. S. Arnold, P. Loan, A. Habib, C. T. John, E. Guendelman, and D. G. Thelen, "Opensim: open-source software to

create and analyze dynamic simulations of movement," *IEEE transactions on biomedical engineering*, vol. 54, no. 11, pp. 1940–1950, 2007.

[42] A. Menegolo, "SimTK: Upper and Lower Body Model," https://simtk. org/projects/ulb_project.

[43] D. G. Thelen, "Adjustment of muscle mechanics model parameters to simulate dynamic contractions in older adults," *J. Biomech. Eng.*, vol. 125, no. 1, pp. 70–77, 2003.

[44] K. R. Holzbaur, W. M. Murray, and S. L. Delp, "A model of the upper extremity for simulating musculoskeletal surgery and analyzing neuro-muscular control," *Annals of biomedical engineering*, vol. 33, no. 6, pp. 829–840, 2005.

[45] F. E. Zajac, "Muscle and tendon: properties, models, scaling, and application to biomechanics and motor control." *Critical reviews in biomedical engineering*, vol. 17, no. 4, pp. 359–411, 1989.

[46] R. L. Lieber and S. C. Bodine-Fowler, "Skeletal muscle mechanics: implications for rehabilitation," *Physical therapy*, vol. 73, no. 12, pp. 844–856, 1993.

[47] C. Lanczos, *The variational principles of mechanics.* University of Toronto press, 2020.

[48] S. S. Stevens, "Problems and methods of psychophysics." *Psychological Bulletin*, vol. 55, no. 4, p. 177, 1958.

[49] L. A. Jones and H. Z. Tan, "Application of psychophysical techniques to haptic research," *IEEE transactions on haptics*, vol. 6, no. 3, pp. 268–284, 2012.

[50] M. Emoto, K. Masaoka, M. Sugawara, and Y. Nojiri, "The viewing angle dependency in the presence of wide field image viewing and its relationship to the evaluation indices," *Displays*, vol. 27, no. 2, pp. 80–89, 2006.

[51] J. Brooke, "System usability scale (SUS): a quick-and-dirty method of system evaluation user information," *Reading, UK: Digital Equipment Co Ltd*, vol. 43, pp. 1–7, 1986.

[52] S. G. Hart and L. E. Staveland, "Development of nasa-tlx (task load index): Results of empirical and theoretical research," in *Advances in psychology.* Elsevier, 1988, vol. 52, pp. 139–183.

[53] C. Raima, M. Ito, S. Saiki, Y. Yamazaki, and Y. Kurita, "Developing a sense of agency scale for heavy machinery operation," in *2020 13th International Conference on Human System Interaction (HSI).* IEEE, 2020, pp. 45–49.

[54] S. Holm, "A simple sequentially rejective multiple test procedure," *Scandinavian journal of statistics*, pp. 65–70, 1979.

[55] N. Hogan, "Adaptive control of mechanical impedance by coactivation of antagonist muscles," *IEEE Transactions on automatic control*, vol. 29, no. 8, pp. 681–690, 1984.

[56] R. Baratta, M. Solomonow, B. Zhou, D. Letson, R. Chuinard, and R. D'ambrosia, "Muscular coactivation: the role of the antagonist musculature in maintaining knee stability," *The American journal of sports medicine*, vol. 16, no. 2, pp. 113–122, 1988.

[57] P. L. Gribble, L. I. Mullin, N. Cothros, and A. Mattar, "Role of cocon-

traction in arm movement accuracy," *Journal of neurophysiology*, vol. 89, no. 5, pp. 2396–2405, 2003.

[58] R. Osu, D. W. Franklin, H. Kato, H. Gomi, K. Domen, T. Yoshioka, and M. Kawato, "Short-and long-term changes in joint co-contraction associated with motor learning as revealed from surface emg," *Journal of neurophysiology*, vol. 88, no. 2, pp. 991–1004, 2002.

[59] J. H. Mitchell, W. Haskell, P. Snell, and S. P. Van Camp, "Task force 8: classification of sports," *Journal of the American College of Cardiology*, vol. 45, no. 8, pp. 1364–1367, 2005.

[60] U. Proske and T. Allen, "The neural basis of the senses of effort, force and heaviness," *Experimental brain research*, vol. 237, no. 3, pp. 589–599, 2019.

[61] B. L. Luu, B. L. Day, J. D. Cole, and R. C. Fitzpatrick, "The fusimotor and reafferent origin of the sense of force and weight," *The Journal of physiology*, vol. 589, no. 13, pp. 3135–3147, 2011.

[62] J. Brooks, T. J. Allen, and U. Proske, "The senses of force and heaviness at the human elbow joint," *Experimental Brain Research*, vol. 226, no. 4, pp. 617–629, 2013.

[63] D. Phillips, P. Kosek, and A. Karduna, "Force perception at the shoulder after a unilateral suprascapular nerve block," *Experimental brain research*, vol. 237, no. 6, pp. 1581–1591, 2019.

[64] F. Monjo, J. Shemmell, and N. Forestier, "The sensory origin of the sense of effort is context-dependent," *Experimental brain research*, vol. 236, no. 7, pp. 1997–2008, 2018.

[65] K. Higashi, S. Okamoto, and Y. Yamada, "Perceived hardness through actual and virtual damped natural vibrations," *IEEE transactions on haptics*, vol. 11, no. 4, pp. 646–651, 2018.

[66] H. Culbertson, J. M. Walker, M. Raitor, and A. M. Okamura, "Waves: a wearable asymmetric vibration excitation system for presenting three-dimensional translation and rotation cues," in *Proceedings of the 2017 CHI Conference on Human Factors in Computing Systems*, 2017, pp. 4972–4982.

[67] S. B. Schorr and A. M. Okamura, "Three-dimensional skin deformation as force substitution: Wearable device design and performance during haptic exploration of virtual environments," *IEEE transactions on haptics*, vol. 10, no. 3, pp. 418–430, 2017.

[68] Z. F. Quek, W. R. Provancher, and A. M. Okamura, "Evaluation of skin deformation tactile feedback for teleoperated surgical tasks," *IEEE transactions on haptics*, vol. 12, no. 2, pp. 102–113, 2018.

[69] Y. Kamikawa, N. Enayati, and A. M. Okamura, "Magnified force sensory substitution for telemanipulation via force-controlled skin deformation," in *2018 IEEE International Conference on Robotics and Automation (ICRA)*. IEEE, 2018, pp. 4142–4148.

Acknowledgment

I wish to thank my advisor, Professor Yuichi Kurita, for his advice, suggestions, encouragement, and patience. He has taught me in the various research fields of biosignal analysis, haptics, human augmentation, and human–machine interfaces. His dedication to research has been a true inspiration.

I am also grateful to committee members Professor Toshio Tsuji and Professor Toru Yamamoto for their invaluable suggestions and opinions on this dissertation.

Thanks also go to Assistant Professor Zu Soh, Tenure-track Assistant Professor Akira Furui, and Project Assistant Professor Swagata DAS for their helpful comments and kind efforts to support my research, my spirit.

I must also take this opportunity to thank Associate Professor Kazushige Koiwai, Associate Professor Masaru Ito, Assistant professor Chiaki Raima for their valuable advice and assistance whenever I needed them.

I am also thankful to all lab members of the Biological Systems Engineering laboratory for their encouragement and support.

I am grateful to Kobelco Construction Machinery Co., Ltd. for providing valuable academic aid during my Ph.D. degree.

Finally, I thank my family and friends for supporting me and giving me the courage to fulfill my desires through this academic degree.